ACS OMEGA

Open Access

http://pubs.acs.org/journal/acsodf

Article

Doxycycline-Loaded pH-Sensitive Microparticles as a Potential Site-Specific Drug Delivery System against Periodontitis

Ardiyah Nurul Fitri Marzaman, Ulfah Mahfufah, Nurul Fauziah, Fadhlil Ulum Ar Rahman, Nasyrah Hidayati, Rafikah Hasyim, Dian Setiawati, Syaiful Choiri, Nur Aisyah Nuzulia, Aqilah Fidya Madani, Maria Mir, Andi Dian Permana, and Karima Qurnia Mansjur*

Cite This: *ACS Omega* 2025, 10, 5668−5685

Read Online

ACCESS | Metrics & More | Article Recommendations

ABSTRACT: A significant obstacle to the healing process of periodontitis is the development of bacterial biofilms within the periodontal pockets. The efficacy of bacterial biofilm therapy is often hindered by the inadequate penetration of antibacterial agents and the nonspecific targeting of bacteria. This study proposes a novel strategy involving the utilization of pH-sensitive microparticles (MPs) of doxycycline (DOX) to enhance biofilm penetration and enable targeted delivery of DOX to infection sites associated with periodontitis. The MPs were developed using a double-emulsion technique with poly(D,L-lactide-*co*-glycolide) and chitosan in a 1:1 ratio. The morphology of DOX-MP exhibits a spherical form with a particle size of 3.54 ± 0.32 μm and a PDI of 0.221 ± 0.02. The DOX-MP also had great encapsulation efficiency (69.43% ± 5.32) and drug loading efficiency (14.81% ± 1.32) with regulated drug release kinetics and accelerated release rates under low-pH conditions. The antimicrobial activity was evaluated against *Escherichia coli* and *Staphylococcus aureus*, and the results indicated the absence of any viable bacterial colonies after 18 h at twice the minimum inhibitory concentration value. Hydrogel-based MPs deliver DOX to the periodontal pocket infection site for ease of use. *In situ* hydrogels used Pluronic F127 and F68 as the main polymer composition and hydroxypropyl methylcellulose as the adhesion polymer. This formulation exhibited a liquid state at room temperature (25 °C) but went through gelation at 36 °C. The formulation also had good mucoadhesive characteristics (42.65 ± 3.53 dyn/cm^2) and good drug permeation at acidic pH in Mueller−Hinton Broth media with the addition of *E. coli* and *S. aureus* bacteria. *Ex vivo* antibacterial activity significantly reduced the microbial count, biofilm quantity, and metabolic activity, confirming the desired antibacterial effect. Hence, the utilization of free drugs and DOX-MPs did not exhibit a notable dissimilarity, showing that integrating the drug into the matrix was not hindering its antibacterial efficacy.

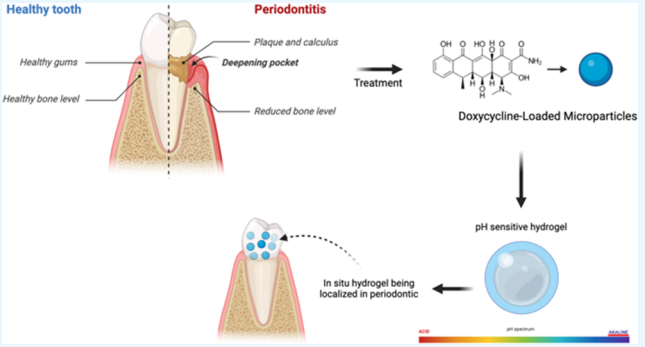

1. INTRODUCTION

Periodontal diseases make up a group of inflammatory conditions affecting the supporting structures of teeth, often resulting in tooth loss if untreated. Periodontitis, driven by complex microbial biofilms, is influenced by factors such as genetics, lifestyle, systemic health, and oral hygiene. It affects up to 50% of the global population and is one of the most prevalent diseases worldwide, posing a significant public health challenge.[1−5] Periodontal diseases are predominantly caused by bacterial biofilm, which is defined as a complex bacterial community attached as aggregates and is enveloped by polysaccharides, adhesive pili, extracellular DNA, lipids, and protein. This self-produced matrix is known as hydrated extracellular polymeric substances (EPS).[6,7] Mitigation strategies for periodontitis traditionally include mechanical debridement, systemic antibiotics, and adjunctive local drug delivery. In recent years, advanced therapies targeting both the microbial and the inflammatory components of the disease have been explored. For instance, stem cell-based strategies have demonstrated potential in promoting osteogenic and angiogenic responses within the periodontal ligament, thereby aiding in tissue regeneration and mitigating disease progression.[8−11] Since the previous century, the chemotherapeutic approach aimed at eradicating pathogens or managing inflammation and antibiotics are a frequently employed treatment option within this approach.[12,13] Antibiotics have limitations when it comes to targeting planktonic bacteria due

Received: October 1, 2024
Revised: January 21, 2025
Accepted: January 28, 2025
Published: February 7, 2025

to their high virulence, potential for multidrug resistance, and the diversity of bacteria phylogroups and serotypes. These limitations can result in the failure to eliminate biofilm bacteria and contribute to antibiotic resistance.[12,14]In addition, developing a novel drug delivery system for periodontitis management that can disrupt and kill the bacterial biofilm is urgently warranted.

Doxycycline hyclate (DOX), as one of several antimicrobial drugs that has been widely used to treat bacterial infections, is capable of killing *Staphylococcus aureus* and *Escherichia coli* by reversibly binding to the 30S ribosomal subunits and preventing the formation of peptide chains of amino acids, which inhibits protein synthesis.[15−18] The development of MPs formulation has been altered by increasing the targeting effectiveness or responding to nearby inducements, such as enzyme, pH, or temperature, in order to increase the effectiveness of the therapeutic substance.[19] The optimization of therapeutic efficacy for periodontitis treatment can be achieved by developing a stimulus-responsive device that can respond to dynamic environmental changes during inflammation including variations in pH levels. The utilization of materials with pH-dependent degradation or solubility features, such as chitosan, may be a viable approach for drug delivery to inflamed periodontal sites, as inflammation is typically associated with a decrease in pH levels.[20,21]

According to a systematic review, systemically administered antibiotics significantly improved the clinical attachment level of the affected teeth.[22] However, systemic drug administration showed disadvantages, including overdosage and adverse effects on the distant organs.[23] To lessen the systemic problems, local distribution using a controlled-release device to directly deliver the antibiotics to periodontal infection areas can be an option.[24] Current approaches for localized drug administration with the utilization of nonbiodegradable ethylene/vinyl acetate fibers or benzoate-containing gels have been developed, but their potential benefits may give rise to certain issues, such as the occurrence of secondary trauma to soft tissue during fiber removal or the release of drugs that cannot be controlled, leading to concentrations that may range from excessive to insufficient.[25,26] A viable option for the treatment of periodontitis is the use of a drug delivery system that employs intrapocket delivery, controlled-release capability, and a bioabsorbable property. Periodontal pockets in this regard serve as a natural reservoir containing gingival crevicular fluid, which facilitates the targeted and controlled release of antimicrobial agents. The objective of using an intrapocket device is to administer an antimicrobial agent in order to attain and sustain a therapeutic drug concentration for the intended duration. The periodontal pathway presents a favorable property for the delivery of sizable, hydrophilic, and unstable proteins, oligonucleotides, and polysaccharides, in addition to conventional low-molecular-weight pharmaceutical compounds.[2] The targeted delivery of drugs to specific drug targets also holds promise for managing and treating periodontal disease by suppressing and eliminating periodontal pathogenic microflora.[27]

In this study, we present the utilization of PLGA microparticles coated with Chitosan for the purpose of encapsulating antimicrobial agents intended for use in intrapocket delivery of periodontitis. Recently, chitosan has been identified as a potential agent for targeting bacterial biofilms due to its reported biocompatibility, biodegradability, and antimicrobial properties.[28,29] Chitosan nanoparticles exhibit a cationic surface charge, while the surfaces of bacterial cell walls and biofilm extracellular polymeric substances (EPS) are anionic. It is expected that chitosan will demonstrate a strong affinity toward areas that are infected.[30]The biocompatibility of poly(lactide-glycolic acid)/poly(d, *l*-lactide-*co*-glycolide) copolymer (PLGA), along with its manageable degradation rate and drug-releasing capacity, make it a popular biomaterial choice for drug delivery systems.[31−33] Leading on from these, the incorporation of chitosan onto PLGA/Chitosan could potentially increase the effectiveness of biofilm targeting.

The objective of this study was to enhance the formulation of PLGA microparticles coated with Chitosan for the purpose of encapsulating a wide-spectrum antimicrobial agent by optimizing the entrapment efficiency (EE), particle size, polydispersity index (PDI), and ζ-potential. In addition, the physicochemical properties of the optimized pH-sensitive microparticles were characterized, and their antimicrobial effectiveness against *E. coli* and *S. aureus* was evaluated. The hypothesis regarding the optimized MPs' ability to release DOX through a pH-triggered mechanism was investigated through controlled-release studies.

The selection of an appropriate dosage form is imperative in order to overcome the possible physical barrier posed by biofilms. This study introduces a novel approach for potentially improving the treatment of periodontitis with bacterial biofilms. Specifically, we developed microparticles (MPs) that contain doxycycline (DOX) and are incorporated into an *in situ* hydrogel. Hydrogel-based MPs were developed to facilitate the site-specific delivery of drugs to sites of infection, ensuring ease of use. The preparation was developed in the form of an *in situ* hydrogel that will form a gel as a result of changes in temperature and release the drug in a sustainable or controlled manner to distribute microparticles through intrapocket delivery. Regarding the formulation, Pluronic F127, has been extensively researched as a pharmaceutical agent that possesses the ability to prolong the retention time of drugs at the site of infection and continuous drug delivery treatment. Additionally, a study utilizing an *ex vivo* antibacterial model was performed to assess the efficacy of this approach. The utilization of DOX-MPs integrated within Pluronic F127 and Pluronic F68 polymers has been demonstrated to yield novel antibacterial therapeutics that exhibit enhanced efficacy in inhibiting the proliferation of *E. coli* and *S. aureus*. The incorporation of hydroxypropyl methylcellulose (HPMC) results in an augmentation of the bio-adhesive properties of the gels on the periodontal pocket. Several *in vitro* and *ex vivo* efficacy tests were conducted along with additional evaluations and characterizations. The outcomes of these proof-of-concept investigations suggest the possible application of this combined delivery method to address the difficulty in treating bacterial biofilm infections in the periodontal pocket.

2. MATERIALS AND METHODS

2.1. Materials. Analytical grade DOX with a minimum purity of 98% was procured from Alfa Aesar (CAS 24390-14-5), located in Lancashire, UK. The procurement of Chitosan (low molecular weight: 50−190 kDa) (CAS 9012-76-4), dichloromethane (DCM) (CAS 75-09-2), and poly(lactic-*co*-glycolic acid) (40−75 kDa) (CAS 26780-50-7) were carried out from Lakeshore Biomaterials (Birmingham, AL). The Pluronic F127 (CAS 9003-11-6) and F68 (CAS 9003-11-6), Tryptone Soy Agar (TSA), and Tryptone Soy Broth (TSB)

https://doi.org/10.1021/acsomega.4c08967
ACS Omega 2025, 10, 5668−5685

medium were procured from Sigma-Aldrich Singapore. The remaining reagents were procured from conventional commercial vendors and were of analytical grade.

2.2. Preparation of Simulated Saliva Fluid (SSF). Preparation of the stock solution of the simulated saliva fluid was made by weighing 37.3 g of KCl, 68 g of KH_2PO_4, 84 g of $NAHCO_3$, 117 g of NaCl, 30.5 g of $MgCl_2(H_2O)_6$ and 48 g of $(NH_4)_2CO_3$. The volumes were calculated to have a final volume of 500 mL for each simulated fluid. The ingredients that have been weighed are then dissolved in an Erlenmeyer flask. To achieve the desired pH, 1 mol/L NaOH and 0.09 mL of HCl were used. Additionally, to achieve the correct electrolyte concentration, the addition of enzymes bile salts, Ca^{2+} solution, and water in the final digestion mixture was needed. The Ca^{2+} solution was achieved by adding 44.1 g of $CaCl_2(H_2O)_2$ to the mixture (Minekus, M. et al. 2014).

2.3. DOX-MPs Preparation. The development of DOX-MPs was conducted using the double-emulsion method. PLGA in different concentrations (Table 1) was dissolved in 5 mL of dichloromethane (DCM) as the organic phase. Figure 1A shows a schematic illustration of DOX-MPs preparation.

Table 1. Composition of DOX Microparticles (%w/v)

	F1	F2	F3	F4	F5	F6
PLGA	50	100	150	100	100	100
doxycycline	50	50	50	50	50	50
chitosan	50	50	50	100	150	200

Furthermore, doxycycline was dissolved in 5 mL of distilled water, the drug solution was poured into the PLGA solution while being homogenized using an Ultra-Turrax T25 basic Ika (Works, Inc., Wilmington, North Carolina) for 10 min at 1000 rpm forming an oil-in-water (o/w) emulsion. The emulsion was then emulsified into 1% PVA solution (20 mL) and then was mixed with Ultra-Turrax T25 basic Ika (Works, Inc., Wilmington, North Carolina) for 10 min at 1000 rpm. After that, the dichloromethane (DCM) was evaporated using a magnetic stirrer at 25 °C and 500 rpm for 4 h. Then, the chitosan was dissolved in 10 mL of 1% acetic acid, and the pH was adjusted using 5 M NaOH to achieve pH 4. The chitosan solution was mixed with the first microparticle dispersion while stirring at 200 rpm for 15 min. The drug that is not absorbed and free of PVA is washed with Milli-Q water using a centrifuge at 5000 rpm. This procedure was performed three times. The resulting MP sediment was dried at 37 °C for further use.

2.4. Microparticles (DOX-MPs) Characterization. *2.4.1. Particle Size and Polydispersity Index Determinations.* In this study, we used a light microscope (Olympus CS33, Olympus Corporation) to observe the size of the particles and calculate the polydispersity index (PDI) values. The microscope was calibrated utilized a 10× magnification Optilab camera.[34]

2.4.2. Percentage of Encapsulation and Drug Loading Efficiency. At room temperature, the DOX-MP suspension was centrifuged at 5000 rpm for 10 min while being dissolved and dispersed in 95% (w/v) acetonitrile. The liquid portion of the sample was extracted and subsequently subjected to analysis using a UV−vis spectrophotometer set at a wavelength of 280 nm. The determination of percentage encapsulation efficiency (EE) and percentage drug loading (DL) of DOX-MPs was conducted through the utilization of the subsequent equations

$$\%\ \mathrm{DL} = \frac{\text{amount of encapsulated drug}}{\text{total weight}} \times 100\% \quad (1)$$

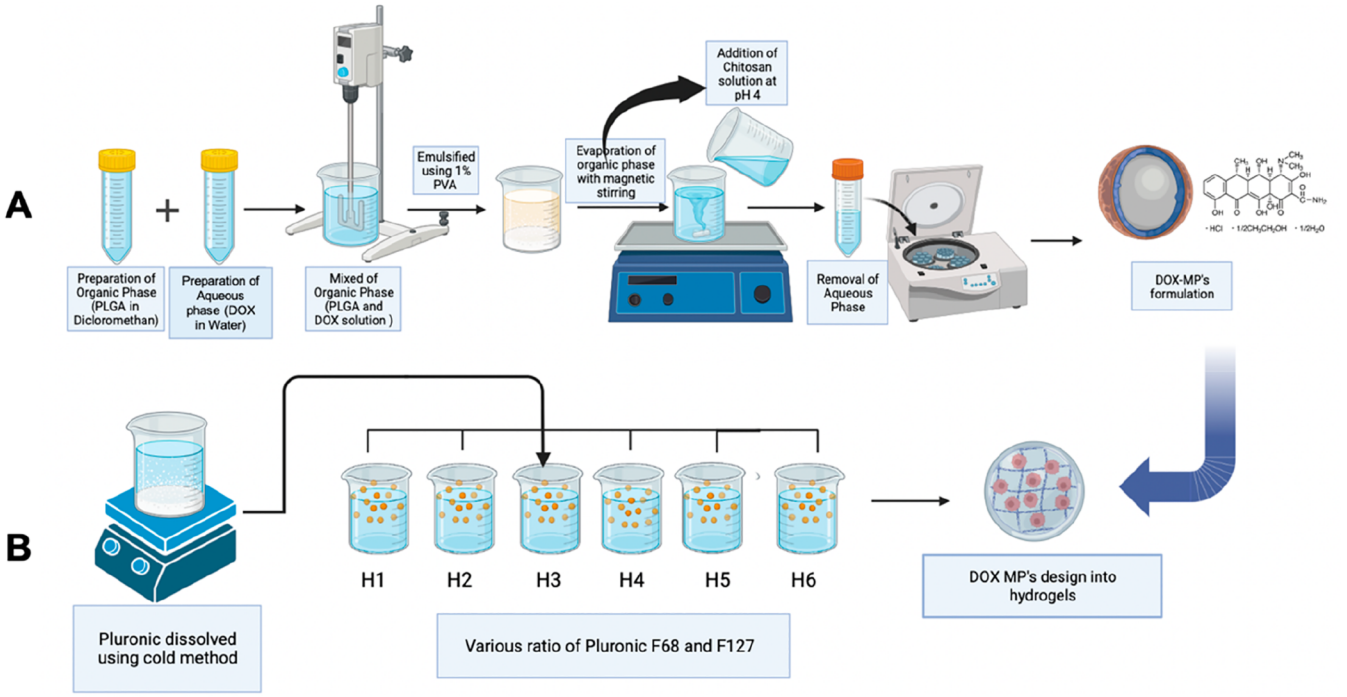

Figure 1. Schematic illustration of DOX-MPs preparation (A) and schematic illustration of DOX-MPs incorporation into hydrogels *in situ* (B). Figure *created using BioRender* (https://biorender.com).

https://doi.org/10.1021/acsomega.4c08967
ACS Omega 2025, 10, 5668−5685

$$\%\ \mathrm{EE} = \frac{\text{drug total} - \text{drug free}}{\text{drug total}} \times 100\% \quad (2)$$

2.4.3. Morphology. The particles were examined using a scanning electron microscope (SEM) with a magnification range of 900−1200 (TM3030 microscope; Hitachi, Krefeld, Germany). Double-sided sticky tape secured the powders to SEM stubs (1 cm in diameter and 1 cm in height) before being coated with gold in a vacuum evaporator.

2.4.4. Fourier Transform Infrared Study. Fourier transform infrared (FTIR) spectrophotometer (Accutrac FT/IR-4100 Series, PerkinElmer, USA), was used to determine the possible interactions between the components of DOX-MPs formulation. Samples of DOX, DOX-MPs, PLGA, chitosan, and the physical mixture of DOX & PLGA/Chitosan (1:1) were run through an FTIR spectrophotometer and scanned in the 400−4000 cm^{-1} wavenumber region.

2.4.5. Differential Scanning Calorimetry. The thermal properties of various formulations, including free drug, DOX-MPs, and a physical mixture of DOX and PLGA/Chitosan (1:1), were evaluated and compared. Curves were generated by utilizing a TGA50H thermobalance (DSC 2920, TA Instruments, Surrey, UK) under controlled conditions of a dynamic nitrogen environment with a flow rate of 100 mL min^{-1}, a heating rate of 10 °C min^{-1}, and a temperature range of 50−550 °C, while utilizing an alumina pan. A quantity of 5−10 mg of sample was utilized for analysis.

2.4.6. X-ray Diffraction (XRD). The formulations were pulverized, arranged, and enclosed with glass. A Shimadzu X-ray diffractometer, manufactured by Rigaku Corporation in Kent, England, was utilized to conduct measurements. Cu Kα1 radiation with a wavelength of 1.54 Å was employed at 30 kV and 30 mA during the process. The samples underwent evaluation at varying angles between 4° and 40° over a period of 2 h, with an incremental increase of 0.02° (equivalent to 1.2° per minute).[35]

2.4.7. Drug Release Kinetics Using Mathematical Modeling. The DOX-MPs in vitro release investigation in bacterial cultures was established. An assessment of the liberation of DOX from MPs matrices under conditions of the presence or absence of bacteria, utilizing simulated saliva fluid (SSF), was evaluated.[36] In summary, MPs with DOX equivalence of 5 mg were homogeneously distributed in 5 mL of bacterial cultures, where the optical density was adjusted to 0.1 at 550 nm. The mixture was then subjected to incubation at 37 °C with constant stirring at 100 rpm using an orbital shaker. Samples were extracted at specific time intervals of 0.25, 0.5, 0.75, 1, 2, 3, 4, 5, 6, 7, 8, and 24 h during the incubation process. Each sample was filtered using an Amicon Ultra Centrifugal Device manufactured by Millipore, Inc., which has a molecular weight cutoff (MWCO) of 12 kDa, and a volume of 0.5 mL was used for each aliquot. The spectrophotometer UV−vis was utilized to determine the concentration of DOX present in the filtrate.[37−39] Several mathematical models were employed to approximate the rate of drug release. Models with R values closer to 1 were selected for mathematical model, as per the following methods[40,41]

$$\text{zero order kinetics: } C_t = C_0 + k_0 t \quad (3)$$

This shows that the release of drug is not influenced by the concentration in the formulation

$$\text{first order kinetics: } \ln C_t = \ln C_0 + K_1 t \quad (4)$$

This shows that the release of drug is linear with the concentration in the formulation

$$\text{Higuchi model: } C_t = k_H t \quad (5)$$

This shows that the release of drugs is controlled by the matrices in the formulation

$$\text{Korsmeyer-Peppas: } C_t = k_{kp} t^n \quad (6)$$

This shows that the release of drugs follows the non-Fickian mechanism from the polymeric system

$$\text{Hixson Crowell (HC): } {C_t}^{1/3} - {C_0}^{1/3} = {K_{HC}}^t \quad (7)$$

This shows that the release of drugs depends on the surface area and particle size of the formulation.

The aforementioned equation delineates the relationship between the percentage of drug released at time t, denoted as C_t (%), the initial value of C_t, denoted as C_0, the time elapsed, denoted as t, the diffusion release exponent, denoted as n, and the release coefficients K_0, K_1, K_H, K_P, and K_{HC}, which correspond to relevant kinetic models. The model parameters were calculated using DD-Solver software.

2.5. In Vitro Antibacterial Activity Evaluation.

2.5.1. Culture of Bacterials. *E. coli* and *S. aureus* (ATCC 25923) cultures purchased from LGC Standards, Middlesex, UK, were maintained at 4 °C. TSA was used to grow bacteria for 24 h and incubated at 37 °C. Bacterial pellets were gathered and reconstituted in sterile water. The optical density was calibrated to a concentration of 1.5×10^7 CFU/mL prior to the antibacterial testing.

2.5.2. Minimum Inhibitory Concentration and Minimum Bactericidal Concentration Determination. Further investigation was conducted on the antibacterial activity of the formulations of free DOX and DOX-MP. The study employed the microtiter broth dilution technique to ascertain the minimum inhibitory concentration (MIC) and minimum bactericidal concentration (MBC) of the test samples in 96-well bottom plates, following the Clinical and Laboratory Standards Institute protocol (Patel et al., 2015). In summary, a bacterial suspension of 100 μL with a concentration of 1.5 × 108 CFU/mL was cultivated in a 96-well plate using their respective medium. The experiment involved the addition of 100 μL of varying concentrations of free drug and DOX-MPs, as outlined in Table 5. Specifically, free drug stock solution was prepared in water, and DOX-MP was prepared in DMSO. This resulted in a final bacterial concentration of 2×10^5 CFU/mL. The microplates underwent incubation at a temperature of 37 °C for a duration of 24 h. The MIC determination was carried out by identifying the final concentrations at which the appearance of TTC color (slightly red) was absent, indicating the suppression of growth. Furthermore, 20 μL dilutions of MIC value and concentrations exceeding MIC were cultivated on tryptic soy agar (TSA) plates and subjected to incubation at 37 °C for an additional 24 h period in order to ascertain the MBC. The MBC was determined as the concentration required to achieve a 99.9% reduction in bacterial viability.

2.5.3. Time Killing Assay of Microparticle. Modified protocols based on previous studies were employed to conduct the time killing assays of DOX and DOX-MPs. The bacterial suspension of *S. aureus* and *E. coli* was standardized to a concentration of 7.5×10^6 CFU/mL through the addition of dilutions of DOX and DOX-MPs at concentrations equivalent to the MIC, twice the MIC, and four times the MIC. Culture

https://doi.org/10.1021/acsomega.4c08967
ACS Omega 2025, 10, 5668−5685

Table 2. Composition of DOX-MPs *In Situ* Hydrogel Formula (%w/w)

	% composition (w/w)					
compositions	H1	H2	H3	H4	H5	H6
DOX-MPs equivalent to 1% drug	1	1	1	1	1	1
pluronic F127	20	15	10	15	15	15
pluronic F68	0	5	10	5	5	5
HPMC	0	0	0	0,5	1	1.5
distilled water	ad 100	ad 100	ad 100	ad 100	ad 100	ad 100

samples of 20 μL were collected at regular intervals of 0, 2, 4, 6, 8, 12, 18, and 24 h and subsequently cultured on TSA plates for cultivation. Subsequently, the enumeration of colony-forming units (CFU) on the TSA plates was conducted after a 24 h incubation period at 37 °C. The curve was obtained by plotting the logarithmic colony-forming units per milliliter (CFU/mL) against the time kill.[42,43]

2.6. In Situ Hydrogel of DOX-MPs Formulation. The *in situ* hydrogel of DOX-MPs was formulated utilizing diverse polymer concentrations of Pluronic F127 and F68, as presented in Table 2. Pluronic F127 and F68 were combined in varying proportions and subsequently refrigerated for a duration of 12 h, as depicted in Figure 1B. The consistent agitation of the mixture resulted in a homogeneous blend, devoid of any visible lumps. The preparation of the formulation involved the dissolution of a mixture of ingredients in water with constant stirring until a transparent solution was obtained. The quantity of HPMC incorporated into the solution was contingent upon the ratios employed, as indicated in Table 2. Subsequently, the *in situ* hydrogels were prepared by utilizing a concentration of 1% DOX-MP, which is equal to 1% of free DOX. All formulations were prepared to achieve a final concentration of 50 mL.

2.6.1. Characterization of In Situ Hydrogel of DOX-MPs.

2.6.1.1. Gelation Temperature (Tsol−gel). The sol−gel transition temperature was determined through a previously described method, wherein 2.5 mL of in situ gel was placed in a closed-tube vial and subjected to heating in a water bath set at 20 °C. When the temperature of the bath was increased by 1 °C, the vials underwent a 90° rotation. The Tsol−gel is the temperature at which the gel exhibits a stop flow when the vial is rotated. The tests were conducted in triplicate (mean ± SD)[44]

2.6.1.2. Mucoadhesion Strength. In this investigation, a modified balancing technique was employed to evaluate the mucoadhesive properties of hydrogel formulations, using a surface area of 2.9 cm^2 and a standardized quantity of 1 g for each sample. At 30 s intervals, a predetermined weight was applied to the right arm of the scale in order to determine how much pressure was needed to release off the gel. The addition of weight to the vials continued until the surface of both vials was separated, at which point of weight, the separation of both vials was recorded and calculated. The study was conducted in triplicate at a physiological temperature of 36 °C. The equation utilized for the determination of mucoadhesive strength is explicated as follows

$$\text{mucoadhesive strength } (N/m^2) = \frac{mg}{A} \times 0.1 \quad (8)$$

where m refers to the mass (gram) needed to release off the gel, g refers to the acceleration due to gravity (980 m/s^2), and A refers to surface area (cm^2).[45]

2.6.1.3. Viscosity. The viscosity of the formulations was measured by using a Brookfield viscometer (NDJ-5S Viscometer) equipped with a spindle that was appropriately sized and set to the appropriate speed. The study involved the experimentation of hydrogels at varying temperatures, specifically 4, 25, and 37 °C. The viscosity of the sample was determined through three independent measurements using spindle 7 at 37 °C and spindle 3 at 4 and 25 °C. The measurements were conducted at a constant speed of 50 rpm with a sample volume of 50 mL.

2.6.1.4. pH Measurement. The pH level of the *in situ* hydrogel formulation plays a critical role in facilitating the targeted delivery of the preparations, owing to the unique feature of pH-sensitive microparticles. The pH levels were assessed in triplicate by means of a digital pH meter (Horiba Scientific, Kyoto, Japan). The acceptability of the application is contingent upon the pH range falling within the appropriate parameters.

2.6.1.5. In Vitro Permeation Study. The in vitro permeation of DOX was evaluated by using the Franz diffusion cell. The cellophane membrane was employed for analytical purposes. The receptor compartment was charged with five distinct media, namely, SSF media at pH 6.8, infected media at pH 5, Mueller-Hinton Broth (MHB) at pH 6.8, MHB with *E. coli*, and MHB with *S. aureus*. A magnetic bar was placed inside the receiving chamber to facilitate stirring. The placement of the membrane occurred between the receptor and donor compartments. The experimental conditions involved maintaining the temperature of the cell at 37 ± 1 °C and subjecting it to agitation by using a magnetic stirrer operating at 100 rpm. A quantity of 1 g of gel formulation was introduced into the donor compartment. Samples of approximately 1 mL were collected at predetermined time intervals of 0.25, 0.5, 1, 2, 3, 4, 5, 6, 7, 8, 12, and 24 h. Following each instance, an equivalent amount of new media was introduced into the receptor compartment to sustain the sink conditions. A UV−vis spectrophotometer (Dynamica, HALO XB-10, UK) was utilized to measure the absorbance of the sample at a wavelength of 231.4 nm. The control assessment involved the evaluation of the in vitro permeation study of the free drug, specifically DOX-only.

2.7. *Ex Vivo* Antibiofilm Activity. The *ex vivo* model was modified to that described by Walkerm.[46] Biofilms were cultured for both Gram-positive (*S. aureus*) and Gram-negative (*E. coli*) bacteria using a 96-well plate. A volume of 0.5 mL of bacterial suspension was combined with 19.5 mL of nutrient broth. Subsequently, a volume of 150 μL of the bacterial suspension was added into each well plate and incubated for a duration of 10 days under anaerobic conditions to facilitate the development of biofilm. The medium was replaced at 48 h intervals. Following the removal of the nutrient media, a volume of 20 μL of the undiluted test substances (free drug and DOX-MPs hydrogel) was administered to the biofilms.

https://doi.org/10.1021/acsomega.4c08967
ACS Omega 2025, 10, 5668−5685

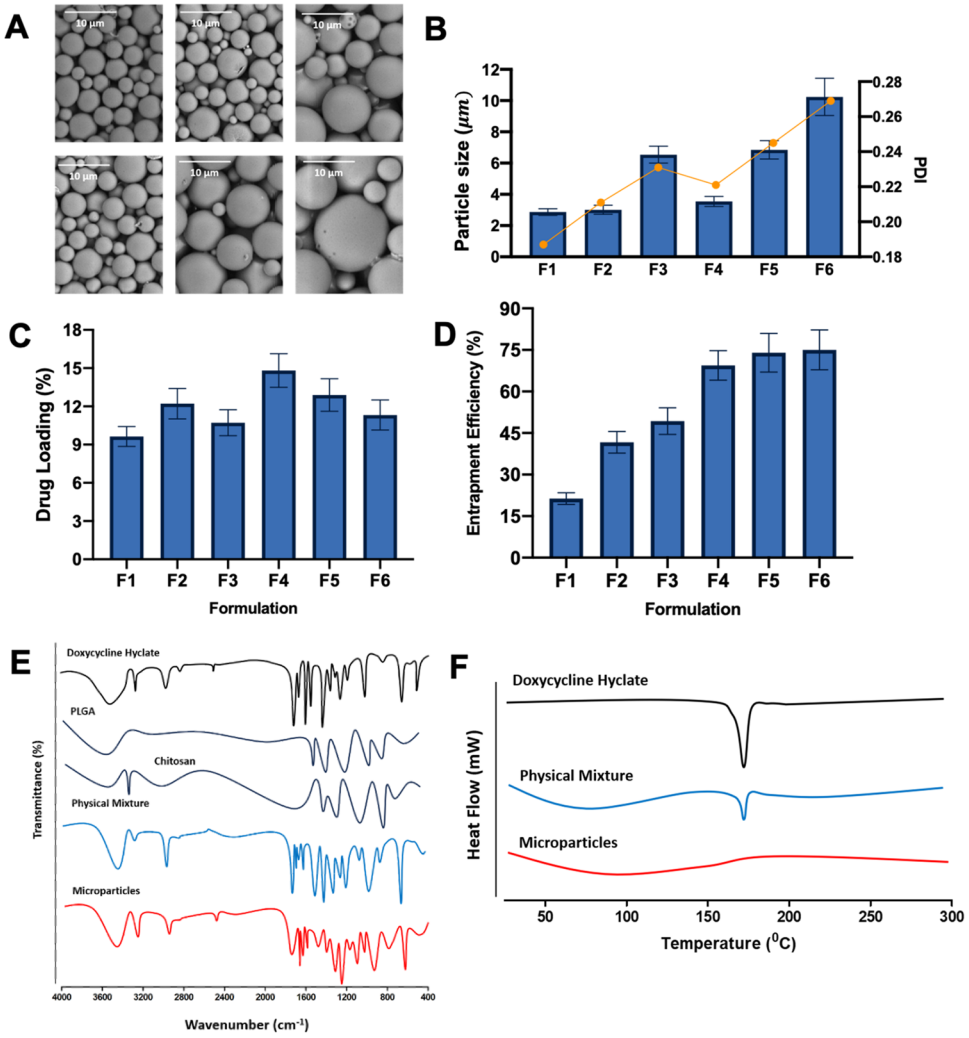

Figure 2. Representative image for scanning electron microscopy (SEM) (A); particle size (B); % drug loading (C); % EE (D), FT-IR (E), DSC (F) (The white scale exemplifies a length of 10 μm in SEM measurement).

Subsequently, the bacterial counts, metabolic activity of the biofilm, and quantity of biofilm matrix were assessed. In order to assess the antibiofilm efficacy of DOX-MPs hydrogel and free DOX in an *ex vivo* model, 20 μL of the supernatant obtained from the well plate after 1, 24, and 48 h of application were inoculated into TSA plates and incubated at 37 °C for 24 h. Moreover, a blank hydrogel was administered onto the well plates, and the same procedure was performed. The quantification of colony-forming units (CFUs) of the biofilms was ultimately determined according to recently published protocols.[47] Following the rinsing process, the biofilms were subjected to fixation at a temperature of 60 °C for a duration of 60 min. Subsequently, the biofilms underwent staining with 50 μL per well of 0.06% (w/v) crystal violet (Sigma-Aldrich Chemie GmbH) for a duration of 10 min. The evaluation of biofilm metabolic activity was conducted through utilization of Alamar blue as a redox indicator. A volume of 5 μL of Alamar blue (alamarBlue reagent, Thermo Fisher Scientific, Inc., Waltham, Massachusetts) was combined with 100 μL of the nutrient medium and subsequently added into the biofilm. After extensive mixing with the biofilm and incubation for 1 h at 37 °C, absorbance levels were measured at 570 nm using UV−vis spectrophotometry (Dynamica, HALO XB-10, Dynamica Scientific Ltd., UK).[48]

2.8. Statistical Analysis. The statistical data was reported in the format of mean ± standard deviation (SD). The statistical analysis of the data involved the computation of several parameters, including the mean, standard deviation, linear regression analysis, percentage relative standard deviation (RSD), and coefficient of variation. The calculations were performed using Microsoft Excel 2021 (developed by Microsoft Corporation, located in Redmond, USA). The statistical analysis of the data was performed utilizing GraphPad Prism version 6, a software developed by GraphPad Software located in San Diego, California. The results indicate statistical significance at a significance level of 0.05, as evidenced by a p-value of less than 0.05 (p-value < 0.05).

3. RESULTS AND DISCUSSION

3.1. Size, Polydispersity Index, and Encapsulation Efficiency of the Composite Microparticles. The particle size of microencapsulated compounds can offer significant insights into the development of stable formulations. The study determined the particle sizes of DOX-MPs in F1 to F6 to be 2.87 ± 0.21, 3.01 ± 0.29, 6.54 ± 0.54, 3.54 ± 0.32, 6.85 ± 0.59, and 10.24 ± 1.19 μm, respectively. It was found that the increase in polymer concentration could affect the size of particles produced. The increase in polymer amount led to the

https://doi.org/10.1021/acsomega.4c08967
ACS Omega 2025, 10, 5668−5685

Table 3. Specifics Regarding the Formulation Parameters That Went into the Making of DOX-MPs and Their Respective Particle Size, PDI, %EE, and % Drug Loading (Mean ± SD, n = 3)

formulation code	particle size (μm) ± SD	PDI ± SD	EE (%) ± SD	drug loading (%) ± SD
F1	2.87 ± 0.21	0.187 ± 0.01	21.34 ± 2.09	9.64 ± 0.78
F2	3.01 ± 0.29	0.211 ± 0.02	41.65 ± 3.89	12.21 ± 1.19
F3	6.54 ± 0.54	0.231 ± 0.02	49.32 ± 4.78	10.72 ± 1.02
F4	3.54 ± 0.32	0.221 ± 0.02	69.43 ± 5.32	14.81 ± 1.32
F5	6.85 ± 0.59	0.245 ± 0.02	73.98 ± 6.95	12.89 ± 1.27
F6	10.24 ± 1.19	0.269 ± 0.02	75.02 ± 7.19	11.32 ± 1.18

increase in viscosity of the polymeric solution. As such, this decreased the homogenization efficiency, producing a larger particle size.[49] The polydispersity index (PDI) values for all formulations are also depicted in Figure 2B. The observation of MPs exhibiting elevated PDI values suggests a wide-ranging size distribution, thereby implying a greater propensity for Ostwald ripening of the substance. Conversely, a PDI value that is lower and closer to zero indicates that there is a uniform dispersion among particles and a comparatively narrow distribution with robust physical stability. There was no statistically significant difference found between PDI values of F1−F6 ($p > 0.05$).

The percentage of drug loading and encapsulation efficiency show how effectively DOX was encapsulated in PLGA/Chitosan MPs. The study revealed that the encapsulation efficiency was comparatively lower when the concentration of PLGA and Chitosan was reduced (F1−F3). The efficiency percentages of F1, F2, and F3 were 21.34 ± 2.09, 41.65 ± 3.89, and 49.32 ± 4.78, respectively. The observed reduction implies that a certain amount of DOX was not incorporated into the matrix. Samples exhibiting encapsulation efficiencies greater than 60% were identified in F4, F5, and F6, with corresponding EE values of 69.43 ± 5.32, 73.98 ± 6.95, and 75.02 ± 7.19, respectively. The outcomes were influenced by the proportions of PLGA and Chitosan. It was anticipated that an MP system with a high drug loading capacity would require a reduced amount of matrix material during preparation. The drug loading and entrapment efficiency were observed to be significantly influenced by various factors, such as polymer composition, molecular weight, drug−polymer interaction, and the presence of end functional groups (ester or carboxyl). The utilization of ionic interaction between drug and matrix materials has been demonstrated to be a highly efficacious strategy for enhancing drug loading, particularly for small particles.[50] The drug loading process exhibited a statistically significant variance ($p < 0.05$). However, the drug concentration in the microparticle preparation was found to be independent of the polymer ratios. F4 was selected for further evaluations due to its higher drug loading capacity and showed a nonsignificant difference when compared to F5 and F6. The F4 formulation also showed no significant difference between F1 and F2, which showed a smaller particle size, Table 3. In addition to that, the surface topography of the F4 microparticle formulation composed of PLGA and Chitosan was examined using SEM, and the corresponding images are presented in Figure 2A. The morphology of the initial DOX-MPs exhibited a uniform spherical configuration with a smooth surface, which is consistent with the prior findings.[51,52]

3.2. FTIR Evaluation. FT-IR spectra that demonstrate the interaction between PLGA/Chitosan of DOX-MPs, as well as the physical mixture of DOX and PLGA/Chitosan, and free drug (DOX alone) are depicted in Figure 2E. The PLGA particles exhibited a spectral pattern featuring an absorption band within the range of 3500−3400 cm^{-1}, which is associated with hydroxyl stretching. The maximum absorption was observed at 3428 cm^{-1}, indicating the presence of intermolecular and intramolecular H-bonding interactions among the chemical constituents of the MPs.[52] The study conducted by Fialho e Moraes et al. reported the observation of a widened hydroxyl stretching band which showed a reduction in the strength of covalent O−H single bonds that can be attributed to an increase in intermolecular hydrogen bonding between PLGA and other compounds. The outcome of this phenomenon is a more interconnected structure.[53] The symmetric vibrational stretching of C−H single bonds of CH_3 groups of PLGA was observed at 2915 cm^{-1} in all formulations.[52]

The vibrational stretching of carbonyl groups (C═O) from PLGA esters is responsible for the intense peak observed at 1348 cm^{-1} in all formulations.[52] One study reported that certain peaks exhibited increased intensity as a result of complete overlap of absorption between various compounds in the formulation.[54] The higher intensity observed at the peak of 3306 cm^{-1} can be attributed to the overlapping of the N−H vibrations of the primary amine from Chitosan.[55] This peak also corresponds to the C═O vibration of PLGA, which was previously described. The DOX-MPs exhibited a higher peak intensity, which may be attributed to the overlapping of the C═C vibration of the benzene ring from the drug components (DOX), similar to the findings of a previous study on trans-cinnamaldehyde components.[56] The absorption peaks in the spectra were observed at 1606 cm^{-1}, which were attributed to the N−H vibrational bending of the secondary amine of chitosan compounds.[57] FTIR spectroscopy findings indicate the intermolecular interactions between the chemical constituents of the MPs, highlighting their strong interactions and compatibility.

3.3. DSC Analysis. Differential scanning calorimetry (Figure 2F) was used to verify the DOX encapsulation within PLGA/Chitosan microparticles. The utilization of this method can serve as an implicit verification of DOX encapsulation within the PLGA/Chitosan matrix. The reason for this phenomenon is that when the active compound is not completely encapsulated, its peaks can be identified on the thermograms of the particles.[58] A narrow endothermic peak was observed in the thermogram of free DOX, occurring at around 181 °C, which corresponds to the melting point of DOX.[51] Moreover, the physical mixture exhibited a similar peak, suggesting the presence of DOX at the particle interface. The thermograms of the PLGA/Chitosan microparticles did not exhibit the DOX peak. Instead, they displayed an endothermic peak, which suggests that DOX was appropriately encapsulated within the MPs and uniformly dispersed throughout the polymeric matrix. This finding was consistent

https://doi.org/10.1021/acsomega.4c08967
ACS Omega 2025, 10, 5668−5685

with a study by Kittur et al.,[59] which revealed that the peak temperature for pure chitosan (181 °C) was higher, indicating that the DOX component was contained inside the MPs and consequently did not display any peak. Furthermore, a greater amount of energy is required to induce the melting of DOX-MPs, due to the alteration of the initial intermolecular structural interactions.

3.3.1. In Vitro Drug Release of DOX-MPs. The objective of this study was to formulate MPs containing DOX for targeted delivery to infected sites. Subsequently, an examination was conducted to evaluate the release behavior of DOX from its MPs compositions, both in the presence and absence of bacterial cultures. Two distinct bacterial strains (*E. coli*) and (*S. aureus*) were chosen and suspended in MHB media. The current methodology utilized simulated saliva fluid (SSF). The graphical representation in Figure 3 illustrates the total

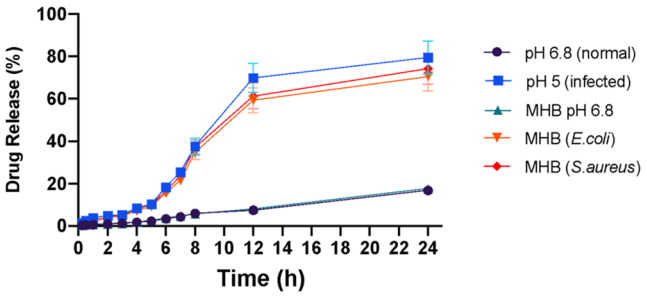

Figure 3. Drug release percentage of DOX-MPs at five different media.

percentage of DOX released through the use of five distinct media, each with varying pH levels, for a duration of 24 h. The results depicted in Figure 3 demonstrate a statistically significant improvement ($p < 0.05$) in the release of DOX from MPs in the presence of bacterial cultures, as compared to the release profiles observed under normal pH conditions in the absence of bacterial cultures. These findings suggest the successful achievement of on-demand delivery of the formulations. The presence of bacterial cultures in the release media did affect ($p < 0.05$) the release behavior of DOX solutions (higher than 60% after 12 h and approximately 80% of drug released after 24 h).

The results showed that the release of drug was dependent on the low pH value, considering that the presence of bacteria leads to a decrease of pH value. This is in line with the chosen delivery option of the formulation through the periodontal pockets. It is known that the intrapocket part of the teeth structure acts as a natural reservoir filled with gingival crevicular fluid and is a good environment for bacterial colonization. Due to these properties, intrapocket drug delivery could maintain the controlled-release delivery of antimicrobials directly to the infection site and avoid the nonspecific release to uninfected areas. The objective of utilizing an intrapocket device for the administration of an antimicrobial agent is to attain and sustain a therapeutic drug concentration for the intended duration. The results of the observation indicate that DOX-MPs exhibited the maximum release at pH 5.0, with a release rate of nearly 70% of the initial DOX quantity in the sample within a duration of 12 h. At the 30 min mark, the quantity of DOX discharged by MHB (*S. aureus*) was greater in comparison to MHB (*E. coli*). In general, the release of drug can be explained by the release of the DOX located close or attached to the particle shell surface.[60]

The inclusion of chitosan in the composition of the MPs resulted in an expedited release of DOX, particularly in environments with lower pH levels. According to Huang et al., the protonation of the chitosan component of the MPs below its pK_a results in increased solubility, swelling, and erosion of the chains.[52] These factors collectively contribute to the rapid release rate obtained from the evaluation of the different media. Consistent with expectations, the findings indicate that the sample coated with chitosan is contingent upon pH, owing to the heightened solubility of chitosan in an acidic environment. The solubility of chitosan in water can be attributed to the presence of a primary amine group in its glucosamine monomeric unit. This group has a low pK_a value of 6.3, causing it to be positively charged and protonated under conditions of low pH. At alkaline pH, the amine group undergoes deprotonation and becomes uncharged, leading to the formation of biopolymeric hydrogel networks that are insoluble. The buffer solution readily permeated the chitosan matrix and established a close interaction with PLGA chains, thereby inducing their swelling and elevating the erosion rate. This leads to a modification in the particle structure, which in turn facilitates the diffusion of the entrapped compound from the particle core.[61,62] As a result, microparticles that were coated with chitosan demonstrated the ability to release elevated levels of drug components. According to Fredenberg et al., the diffusion rate of DOX was found to increase due to the swelling of PLGA chains in solution along with surface erosion, resulting in an increased amount of DOX being released[63] It should be noted that the degradation of PLGA is a gradual process. On the other hand, the use of SSF at a normal pH value of 6.8 and MHB media (pH 6.8) presented a steady-state release profile, keeping the cumulative DOX amount constant and stable during the whole period. The findings indicate that the PLGA/Chitosan microparticles that were developed in this study exhibited varying release patterns based on the environmental pH and the matrix composition. Additionally, it was observed that pH-sensitive polymers, such as chitosan, can stimulate and augment the release process. In addition to the effect of pH, it has been reported that chitosan and PLGA could be easily degraded by lipase enzymes secreted by several bacteria, including *S. aureus* and *E. coli*.[64,65] Therefore, the selective release of DOX could be potentially affected by the pH and properties of the polymers used in this study.

As a biodegradable, biocompatible, and nontoxic polymer, PLGA is also known for its capacity to be highly effective at encapsulating a wide range of hydrophobic molecules and releasing them under controlled conditions, which has led to its high interest as a base polymer for the production of particles for delivery systems.[66] Therefore, the integration of polyelectrolytes, specifically Chitosan, onto a PLGA surface has been shown to improve its stability, cellular uptake, targeting abilities, and regulation of drug release via the pH-triggered ability of Chitosan[52]

Additionally, five different kinetic models were used to examine the drug release data in order to look into how DOX-MPs dissolve in various media and how their kinetics change as they dissolve. The model exhibiting the greatest coefficient correlation was selected as the optimal fit for the release procedure. The study findings indicated that the DOX-MPs release profiles when dissolved in MHB with *E. coli* and *S.*

https://doi.org/10.1021/acsomega.4c08967
ACS Omega 2025, 10, 5668−5685

Table 4. Representative Kinetic Model of Drug Release between Free Drug and DOX-MPs

kinetic model	pH 6.8 (normal)	pH 5 (infected)	MHB pH 6.8	MHB with *E. Coli*	MHB with *S. aureus*
ZO	0.982 240 372	0.878 341 921	0.985 279 926	0.888 961 954	0.896 015 001
FO	0.974 505 4	0.831 676 998	0.977 137 888	0.866 060 028	0.867 074 335
Higuchi	0.705 842 781	0.694 523 421	0.707 315 61	0.694 937 1	0.705 854 994
KP	0.886 444 083	0.800 254 041	0.892 472 659	0.844 801 284	0.853 883 883
HC	0.977 379 048	0.877 584 172	0.980 181 522	0.891 319 96	0.898 064 667

aureus values were consistent with the Hixson−Crowell model. Conversely, the release profiles at normal pH adhered to zero-order models with R values exceeding 0.98, as presented in Table 4. The Hixson−Crowell kinetic models are utilized to elucidate the phenomenon of particle liberation from systems that undergo alterations in particle surface area and diameter. An equation was derived to express the dissolution rate of a drug composed of particles of uniform size, which is dependent on the matrices' erosion capacity to release the drug. Therefore, defining the release pattern of a drug is crucial as it determines the effectiveness of the dosage form. In summary, it can be stated that the drug release process of DOX that is loaded with polymer matrices (PLGA/Chitosan) adheres to an erosion mechanism.[67,68] The study by Fredenberg et al. found that diffusion, including diffusion through pores and polymers and osmotic pumping, is also the main driving force behind the release mechanism.[63] This diffusion is facilitated by the potential chemical difference between the particle's core and its surroundings. Upon being suspended, PLGA undergoes hydrolysis, leading to the liberation of the enclosed substance alongside the byproducts of lactic acid and glycolic acid monomers. The endogenous nature and easier metabolism via the Krebs cycle render these compounds suitable for employment in drug delivery and biomaterial contexts with a high degree of safety medication.[68]

Statistical analysis shows that DOX-MPs dissolved in acidic pH media with the presence of bacteria such as *E. coli* and *S. aureus* have a considerably greater percentage of dissolution profiles compared to when it dissolved in normal pH media ($p < 0.05$), this can be clearly seen in Figure 3.

3.4. *In Vitro* Antibacterial Activity. *3.4.1. MIC and MBC Evaluation.* A further study was conducted on the antibacterial activity of formulations containing free DOX and DOX-loaded MPs. Table 5 presents a comparison of the MIC and MBC values between the DOX solution and its MP formulations. The present study utilized two distinct bacterial strains, one representing Gram-positive and the other Gram-negative bacteria, to evaluate the efficacy of doxycycline MPs. The results demonstrated promising antibacterial activity, with MIC and MBC values of 12.5 and 25 μg/mL, respectively. The results indicated that the DOX PLGA/Chitosan microparticles developed in this study exhibited efficacy against both Gram-positive and Gram-negative bacteria, as evidenced by the equivalent MIC and MBC values observed for both microorganisms. In Gram-negative bacteria, the hydrophilic lipopolysaccharide membrane typically provides protection against hydrophobic substances, such as Doxycycline, thereby increasing their resistance to antimicrobial agents. However, this study did not observe such behavior. Moreover, upon initiation of PLGA hydrolysis, the liberated compounds include lactic and glycolic acids. The reduction in pH levels leads to an elevation in DOX-MPs, which exhibits pH sensitivity. This facilitates its enhanced distribution across the lipid membrane of the cell and enables it to interact with the hydrophobic domains of membrane proteins.[58,69] Furthermore, the employment of encapsulation in PLGA facilitates a more uniform dispersion of the hydrophobic antimicrobial agent throughout the hydrophilic medium.[70] Clearly, the encapsulation of DOX was proven to be effective against both bacteria, and the results were confirmed by a different study that found a similar effect for other hydrophobic antimicrobials that were encapsulated using PLGA.[51,58,71]

Table 5. MIC and MBC of DOX-MPs against *E. coli* and *S. aureus* Bacteria; (+) Shows Growth of Bacteria and (−) Shows No Growth of Bacteria, ($n = 3$)

	E. coli		*S. aureus*	
concentration (μg/mL)	MIC	MBC	MIC	MBC
3.125	+	+	+	+
6.25	+	+	+	+
12.5	−	+	−	+
25	−	−	−	−
50	−	−	−	−
100	−	−	−	−
200	−	−	−	−

Observational evidence suggested that chitosan played a role in the low MIC and MBC values that were achieved. According to the research conducted by Pola et al.,[72] Chitosan exhibited an innate mechanism that enhanced its interaction with the bacterial cell wall, thereby safeguarding the MPs and producing a synergistic effect. The previous study claimed that the mechanism of Chitosan's impact on microbial cells is predicated on an electrostatic affinity between the positively charged amino groups of Chitosan and the negatively charged constituents of the bacterial cell wall.[73] On the other hand, Kong et al. have reported that the mechanism of Chitosan's action on bacterial cells is influenced by the pH of the environment.[74] At a pH below $pK_a \sim 6.3$, the predominant mode of action is through electrostatic interactions, while at higher pH levels hydrophobic and chelating effects become more significant. The authors found that the former mode of action is more effective, and this was also observed in the present study. In addition to its impact on PLGA microparticles, whereby it improves their stability and promotes their interaction with bacterial cells, Chitosan has also been found to be associated with increased DOX release at infection site pH levels, which in turn is linked to improved antimicrobial efficacy. The bacteriostatic effect observed in another study which may be attributed to the rapid and sustained release of DOX from the enclosed particles during the initial hours, which extended the adaptation period necessary for bacterial growth and prevented any potential recovery mechanism by the bacteria[72]

3.4.2. Time Killing Assay (TKA). 3.4.2.1. TKA of Free Drug (DOX-only). In an attempt to explain the time required by

https://doi.org/10.1021/acsomega.4c08967
ACS Omega 2025, 10, 5668−5685

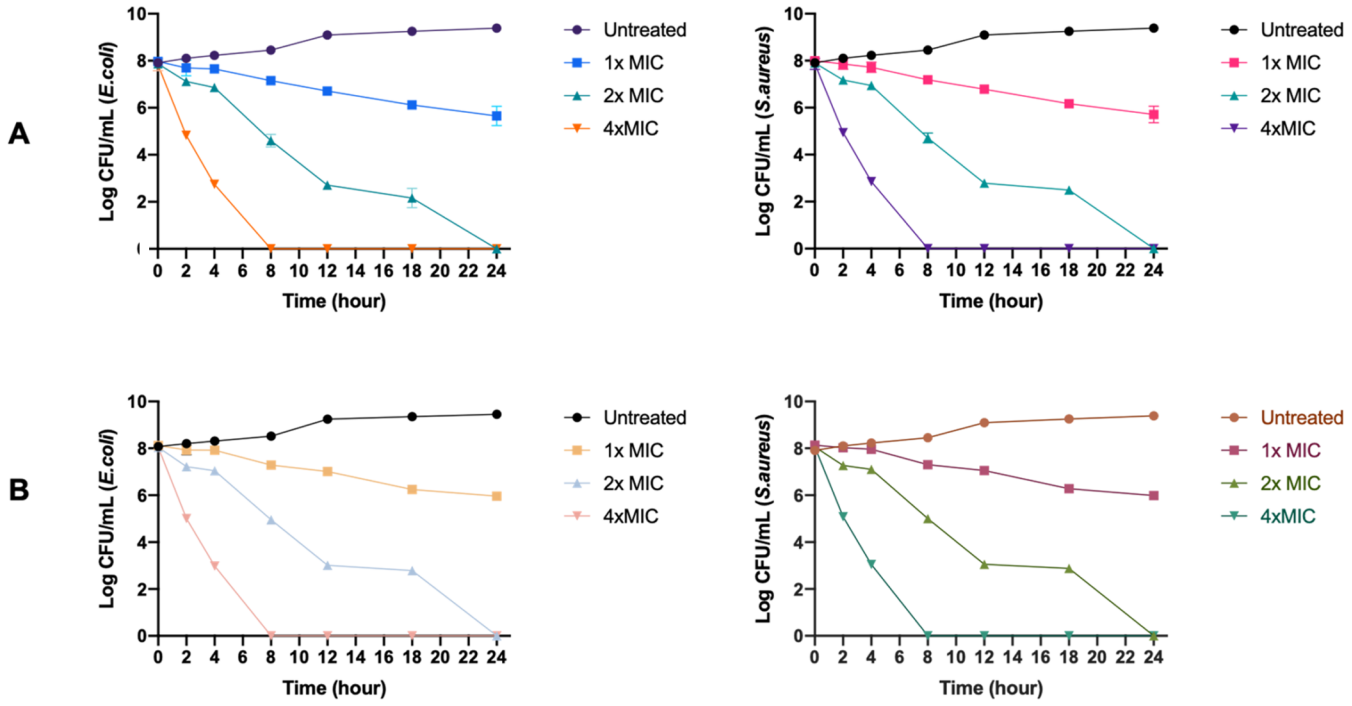

Figure 4. Time killing assay results for (A) free drug (DOX) and (B) DOX-MPs. Data are expressed as the mean ± standard deviation (n = 3). Statistical significance was assessed using one-way ANOVA, and p-values are indicated where appropriate.

DOX and DOX-loaded MPs to kill the bacterial strains tested, time killing assays were carried out. This information was gathered for the purpose of determining whether or not the MPs formulation possessed antibacterial properties. Figure 4A shows free drug of doxycycline time kill curves against *E. coli* and *S. aureus* in terms of time. Following 24 h of growth, the viable bacterial colony in the untreated group reached 9.38 ± 0.08 log CFU/mL.

3.4.2.2. TKA of DOX-MPs. In this study, we determined how long it took for an antibacterial treatment (DOX-MPs) to eradicate bacterial growth completely. Figure 4B demonstrates that after 24 h of incubation with 2× MIC, DOX-MPs showed no signs of viable bacterial colony. In addition, a concentration that was four times higher than the MIC led to a quicker killing time, which was observed after 8 h of incubation for both *E. coli* and *S. aureus* bacteria. Based on these findings, it appears that the antibacterial activity of DOX increases with increasing concentration and prolonged exposure (the degree to which it is dependent on the concentration and the amount of time). Because of its prospective use as an antibacterial agent, the soluble nature of DOX in bacterial growth media was particularly emphasized. It is important to note that in this study, as mentioned in the method, all compounds were completely dissolved in the appropriate solvent. Considering the results that there was no significant difference in the antimicrobial activity between the free drug and DOX-MP, it was shown that the formulation of MPs did not influence the antimicrobial activity of DOX.

3.5. *In Situ* Hydrogel of DOX-MPs Characterization.

The *in situ* hydrogel was formulated using a tripolymer blend consisting of Pluronic F127, Pluronic F68, and HPMC and coded with H1 to H6. Gel formation depended on the ratio of polymer used in the formulation. *In situ* hydrogel properties such as gelation temperature (Tsol−gel), mucoadhesion strength, pH, viscosity, and *ex vivo* drug permeation were investigated.

3.5.1. Gelation Temperature Evaluation (Tsol−gel). The temperature at which gelation occurs (termed Tsol−gel) was an essential component in this theoretical framework. The accurate administration of dosage can be ensured through the employment of an *in situ* hydrogel formulation that retains its liquid state at room temperature and transforms into a gel-like consistency upon contact with the physiological temperature. The optimal temperature range for *in situ* hydrogel was expected to align with the mean oral (salivary) temperature, which falls within the range of 36−37 °C. The determination of the gelation temperature of the liquid was conducted through the employment of the inverted tube technique. The evaluation was done using two types of environments, one without dilution, and the rest using SSF as dilution media, to justify that the presence of saliva in the mouth when the drug was applied would not affect the gelation temperature. Figure 5A shows the illustration of the liquid form when still at room temperature (left) and the gel properties when at oral cavity temperature (right).

3.5.2. Mucoadhesive Strength Evaluation. The length of time the preparation remains available in the mouth has a significant role in determining the drug's bioavailability when it was applied directly to the infection site. To see this effect, adding a certain amount of HPMC within all formulas was evaluated to determine mucoadhesive strength properties. The results of this study are presented in Figure 5C. The mucoadhesive values of DOX-MPs *in situ* hydrogel for H1−H6 (undiluted) were found to be 18.87 ± 1.77, 19.60 ± 1.59, 17.97 ± 1.16, 24.13 ± 2.09, 42.65 ± 3.53, and 64.90 ± 5.59 dyn/cm^2, respectively. On the other hand, the use of SFF as dilution media showed the mucoadhesion of H1−H6 at 17.65 ± 1.61, 18.32 ± 1.34, 16.91 ± 1.71, 23.10 ± 2.10, 40.32 ± 3.76, and 62.34 ± 4.98 dyn/cm^2, respectively. Both evaluations

https://doi.org/10.1021/acsomega.4c08967
ACS Omega 2025, 10, 5668−5685

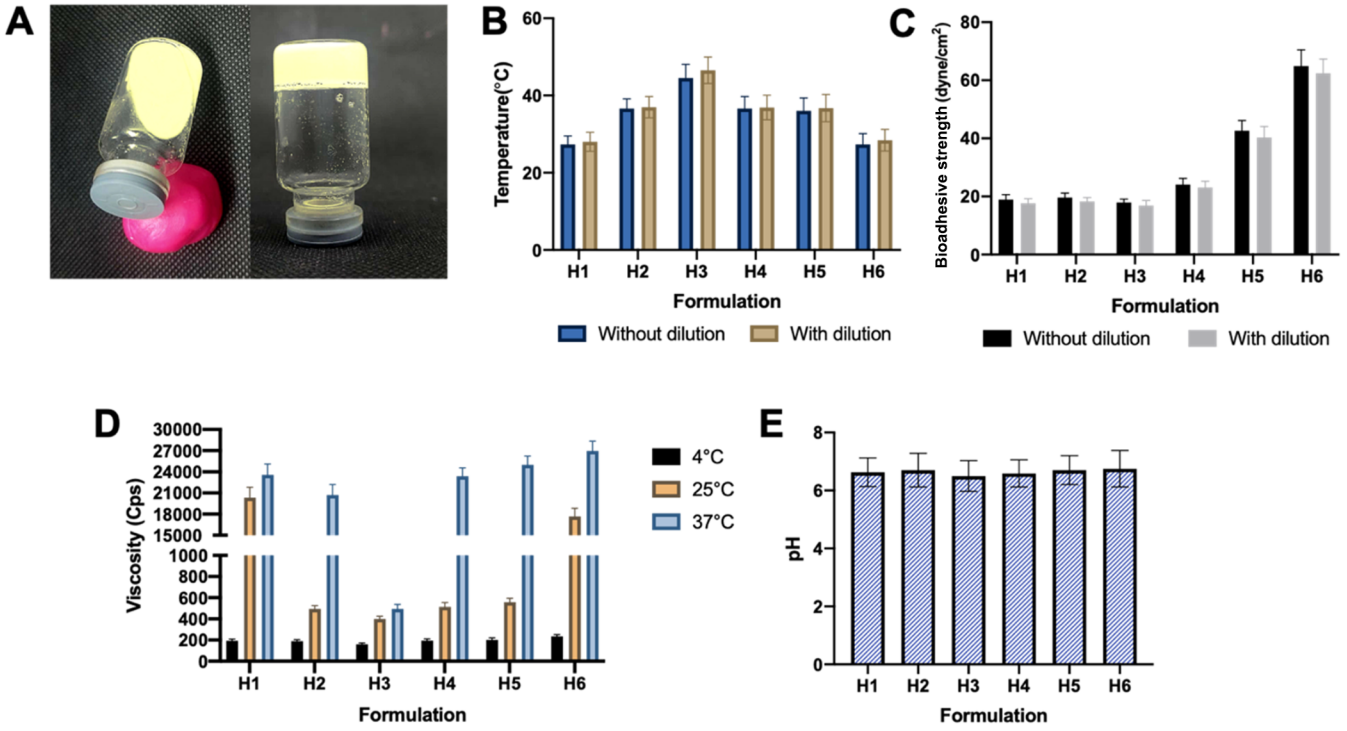

Figure 5. Gelling properties of the formulation at room temperature (left) and at oral cavity temperature (right) (A); gelation temperature (Tsol−gel) (B); bio-adhesive strength (C); viscosity (D); pH value (E). All photographs and data presented in this figure were captured and prepared by the authors. The highest gelation temperature was seen for the H3 formulation at more than 40 °C (panel B), but this formula does not comply with the range of temperature criteria of mouth saliva. The Tsol−gel values of DOX-MPs *in situ* hydrogel formula within H1−H6 for the undiluted evaluation were 27.34 ± 2.18, 36.61 ± 2.50, 44.53 ± 3.52, 36.61 ± 3.10, 36.03 ± 3.36, and 27.33 ± 2.82 °C, respectively. On the other hand, the use of SFF as dilution media showed the gelation temperature of H1−H6 at 28.02 ± 2.43, 36.98 ± 2.76, 46.54 ± 3.44, 36.89 ± 3.19, 36.74 ± 3.54, and 28.41 ± 2.79 °C, respectively. The gelation temperature of both evaluations did not show any significant change, which concludes that the presence of saliva will not affect the gelation temperature. When compared to all formulations, H2, H4, and H5 showed a gelling temperature based on the criteria, while H1 and H6 showed a lower degree of gelation temperature. The results were significantly affected by the ratio of Pluronic F127 to F68 used in the formulation, where the ratio of Pluronic F127 to F68 in H5 was 3:1, respectively. As opposed to Pluronic F68, which is mostly made up of two side PEO blocks and a central PPO block, this occurred as a result of the structural differences between Pluronic F127 and F68. Pluronic exhibits gelation at a specific concentration and temperature, wherein the hydrophobic PPO block undergoes dehydration while the hydrophilic PEO block remains hydrated. The alteration of the PPO/PEO ratio has an impact on the temperature at which gelation occurs. Incorporating a hydrophobic PPO block is expected to result in a reduction of the Tsol−gel. Furthermore, the incorporation of a hydrophilic PEO block results in an elevation of the gelation temperature.[75] It is important to note that HPMC took a role in the sol−gel transformation due to its significant impact on the thermo-reversible behavior. It is common knowledge that the hydrophobic interaction of HPMC chains leads to intermolecular interactions that form sol−gel transformation.

also did not show any significant difference, this can be concluded that again saliva had no impact on the gelation temperature as well as the mucoadhesive properties within all formulas. It can be seen that H5 and H6 had higher bio-adhesive values with HPMC concentrations of 1 and 1.5%, respectively. The gel formulations' mucoadhesive and gelation temperature properties were notably impacted by the presence of HPMC. The mucoadhesive strength increased along with the presence of HPMC in the formulation. In addition, it was observed that the mucoadhesive properties of gels without a mucoadhesive agent (H1−H3) were lower to those of gels containing HPMC. The strength of hydroxyl contacts between Pluronic F127/F68 and the mucosal layer was comparatively weaker in the absence of HPMC, as opposed to when the polymer was combined with HPMC to create an *in situ* gel. The adhesive characteristics of HPMC were also attributed to the phenomenon of hydrogen bonding present from the Pluronic F127/F68.[76,77] Therefore, H5 formulation was chosen as the best formula fitted with the temperature range of the mouth and had good properties of bio adhesivity, even though H6 showed a higher bio-adhesive value but its gelation temperature was lower, forming a gel at room temperature. As a result, this will help to improve the effectiveness of preparations that would be administered via intrapocket delivery.

3.5.3. Viscosity Study. *In situ* gel preparations typically take the form of a solution at room temperature, but they have the ability to change into a gel under specific physiological conditions, which becomes their desirable characteristic. The administration of the preparation in the form of a solution can aid in ensuring the precision of the dosage. Therefore, it is necessary to assess the viscosity between the gel *in situ* formulation at the storage temperature and the temperature that is physiologically suitable for intrapocket administration. The present investigation involved the measurement of viscosity under three distinct conditions, namely, 4 °C to represent cold temperature, 25 °C to represent room temperature, and 35 °C to represent mucosal temperature. The gel formulations' low viscosity at cold and room temperatures is a crucial indicator of their tendency toward the liquid state. It was found that, the rationale behind the requirement for *in situ* gels to exhibit gel-like properties at oral

https://doi.org/10.1021/acsomega.4c08967
ACS Omega 2025, 10, 5668−5685

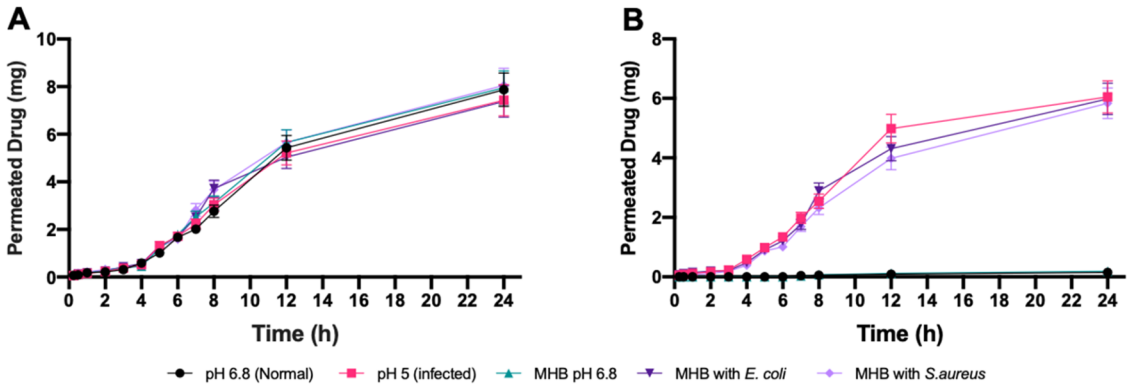

Figure 6. Permeated drug of DOX-only (A) and permeated drug of DOX-MPs (B) (mean ± SD, n = 3).

mucosal temperature for enhanced localization time, while maintaining a free-flowing viscosity at room temperature to facilitate ease of application could potentially reduce the growth of certain bacteria at the infection site.[34,78] The viscosities properties are depicted in Figure 5D. It is observed that the viscosity of H3 compared to the other formula was statistically ($p < 0.05$) different in the mucosal temperature, while that in H1, H4, and H5 showed no significant difference. The addition of HPMC in the formulation also contributes to the increase of viscosity, by seeing the H5 and H6 with HPMC concentration at 1 and 1.5%, respectively, resulting in a higher viscosity value at the mucosal temperature. The results were supported by previous research which showed that higher addition of polymer concentrations also contributes to the viscosity of the preparation due to a rise in temperature-induced intermolecular interactions between HPMC and Pluronic.[79,80] The present study provides further evidence supporting the advantages of utilizing a combination of Pluronic F127 and F68 in conjunction with HPMC for the development of *in situ* gel formulations. This approach effectively facilitates the targeted viscosity during both storage and application at mucosal temperature. Therefore, all of the gels that were tested for the mucosal temperature also exhibited pseudoplastic behavior.

3.5.4. pH Measurement. The gel's intended pH level should be fulfilled by the doxycycline pH-sensitive microparticle (DOX-MPs) formulation. Drug delivery systems were developed to be applied within the natural pH range of approximately 6 in mucosal tissues with the aim of achieving maximum effectiveness and promoting patient adherence to treatment protocols. The alteration in pH values over the duration of a product's storage period may indicate a potential issue with its stability; therefore, it is necessary to maintain its pH in the desired range. Based on the evaluation, there was no statistically significant difference ($p > 0.05$) observed in the pH values among all the formulations, as depicted in Figure 5E. Given that all formulations were within the pH range of 6, it was unnecessary to make any additional pH adjustments for intrapocket delivery as the pH levels were already deemed safe.[81]

3.5.5. In Vitro Permeation Studies. The *in vitro* permeation study was done using a free drug of DOX and DOX PLGA/Chitosan MPs after 24 h in five different media. Figure 6A shows the permeated amount of free drug of doxycycline. It can be clearly seen that the permeated drug was similar in all five different media, which did not show any significant difference ($p > 0.05$). Therefore, the release mechanism of DOX-free drug was not sensitive to the pH condition. Moreover, Figure 6B shows the amount of *in vitro* drug permeated from the DOX-MPs preparation.

The results showed that the release of drug was dependent on the low pH value, found in SSF media at pH 5 (infected), MHB (*E. coli*), and MHB (*S. aureus*). It was considered that the presence of bacteria leads to a decrease of pH value. The amount of DOX permeated from the microparticle hydrogel formulation after 24 h was 6.05 ± 0.54 mg for infected media at pH 5; 5.98 ± 0.53 mg for MHB media with *E. coli*; and 5.84 ± 0.52 mg for MHB with *S. aureus*, while in SSF media at pH 6.8 and MHB media at pH 6.8, a small amount of drug was permeated only after 7 h administration, with the highest achieved at only 0.15 ± 0.01 and 0.19 ± 0.02 mg for SSF pH 6.8 and MHB 6.8 media, respectively. According to the results, this approach was successful in developing pH-sensitive MPs to make it localized in the site of infection for potential intrapocket delivery to treat periodontitis infection. The data were further calculated for the mathematic models. The kinetic models of DOX-MPs followed the HC release mechanism in the presence of *E. coli* which then confirmed that the release followed the erosion mechanism. These findings show that the permeation of DOX-MPs can be improved by making it sensitive to the change of pH and incorporating them into the *in situ* hydrogel formulation.

3.6. Antibacterial Activity in *Ex Vivo* Infection Model.

3.6.1. Microbial Counts from Biofilm Formation. The purpose of the present study was to evaluate the activity of DOX-MPs hydrogels compared to free drug of DOX and control on an *ex vivo* biofilm using *E. coli* and *S. aureus* as the representative for Gram-positive and Gram-negative bacteria.

The colony-forming unit (CFU) counts are given in *E. coli* biofilms without exposure to antimicrobials were 6.76 ± 0.25 log CFU/mL after 60 min, 7.05 ± 0.32 log CFU/mL after 24 h, and 7.32 ± 0.39 log CFU/mL after 48 h. While that in *S. aureus* the amounts of bacteria without the drug exposure were 5.95 ± 0.43 log CFU/mL after 60 min, 6.43 ± 0.39 log CFU/mL after 24 h, and 6.98 ± 0.41 log CFU/mL after 48 h. Compared to when the biofilms were exposed to antimicrobials of DOX-free drug and DOX-MPs, the counts of *E. coli* in biofilms were significantly reduced to 4.32 ± 0.27 (60 min), 3.65 ± 0.18 (24 h), and 2.18 ± 0.09 log CFU/mL (48 h) for DOX-MPs, and 4.19 ± 0.28 (60 min), 3.54 ± 0.17 (24 h), and 2.07 ± 0.08 log CFU/mL (48 h) for free drug of DOX. However, the microbial count for both DOX and DOX-MPs showed no significant difference. Therefore, the formulation of DOX-MPs incorporated into hydrogel did not interfere with

https://doi.org/10.1021/acsomega.4c08967
ACS Omega 2025, 10, 5668−5685

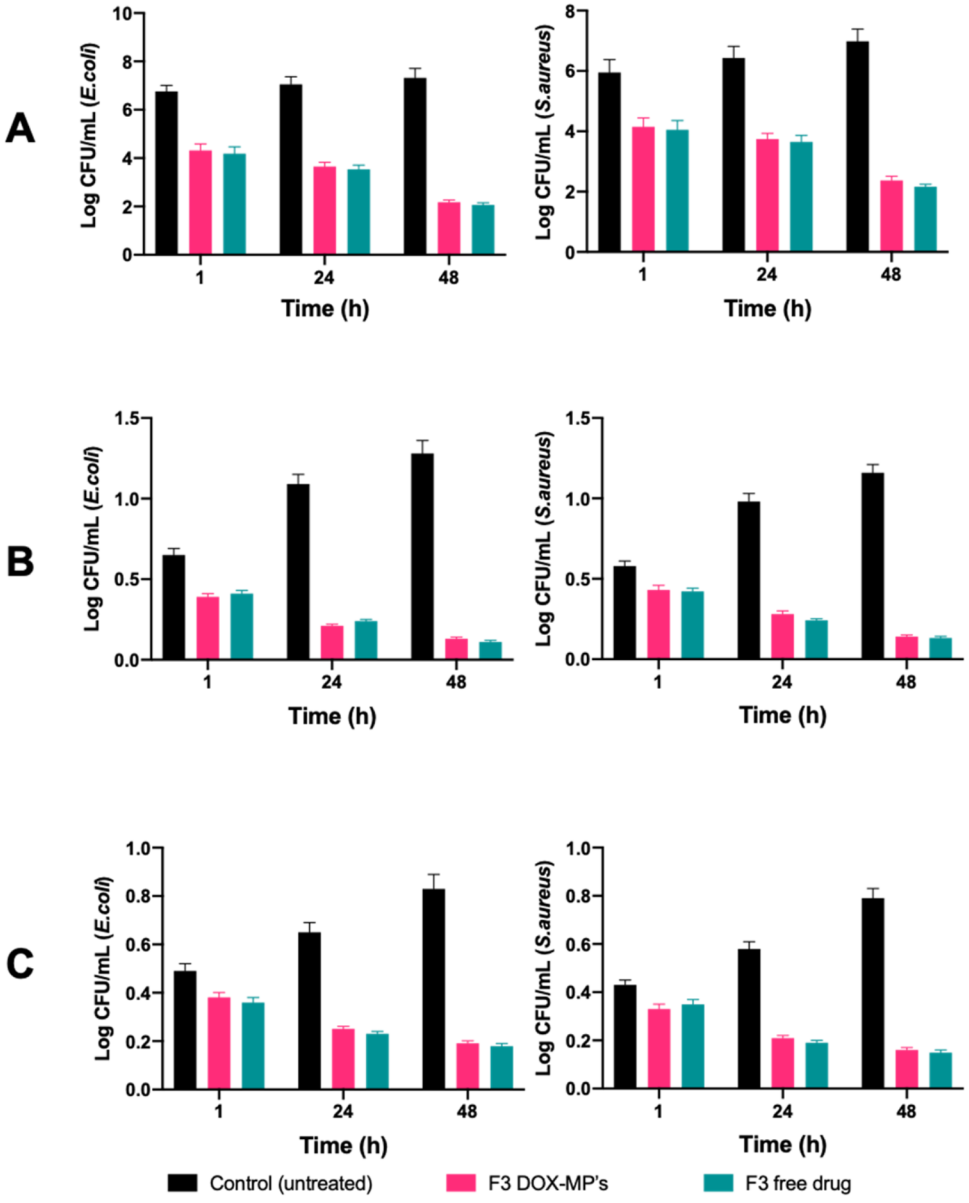

Figure 7. Biofilm microbial count (A); biofilm quantity U (extinction at 594 nm) (B); and biofilm metabolic activity ratio (*U* at 595/570 nm) (C).

the antibacterial activity of the main properties of doxycycline. Compared to the untreated group after 48 h, the highest reduction of biofilm activity after the application of antimicrobials was 89.84% achieved by DOX-MPs. The findings indicate a consistent elevation in bacterial counts, as well as an increase in both biofilm quantity and metabolic activity in the untreated group compared to the treated group (free drug and DOX-MPs), thus confirming the successful establishment of these microorganisms into the biofilms.

3.6.2. Biofilm Quantity and Metabolic Activity. Biofilm consists of a self-produced matrix of extracellular polymeric substances. Interference with bacterial matrix components is an approach in the development of antibiofilm drugs.[82] In this procedure, the biofilm quantity was determined by crystal violet staining. Same as the previous evaluation, this procedure also involved control (untreated), free drug, and DOX-MPs in the analysis. Both treatments significantly reduced biofilm quantity compared to the untreated control. After 24 h, the calculated biofilms of *E. coli* were 0.21 ± 0.01 for DOX-MPs and 0.24 ± 0.01 for DOX-only. The reduction was lower when observed at 48 h, with the calculated biofilm being 0.13 ± 0.01 for DOX-MPs and 0.11 ± 0.01 for DOX-only. In addition to that, metabolic activity in biofilms of *S. aureus* was significantly reduced after 60 min of drug exposure, 0.33 ± 0.02 for DOX-MPs and 0.35 ± 0.02 for DOX-only. The metabolic activity was both *E. coli* and *S. aureus* biofilm was always lower after any antimicrobial's application than in the control without exposure to antimicrobials (Figure 7C). Regarding the amount of biofilm and metabolic activity, the two antimicrobials (DOX-MPs and free drug) did not significantly differ from one another in the current investigation. Both gels exhibit a reduction in biofilm metabolic activity within 60 min, indicating that a lower concentration of doxycycline may be effective in inhibiting bacterial metabolism. In the previous study, it is also seen that the use of vehicle in the gel preparation had no influence on the bacterial counts.[83] All of these data seem to point toward the possibility that doxycycline can be a useful antibacterial medication for the

https://doi.org/10.1021/acsomega.4c08967
ACS Omega 2025, 10, 5668−5685

treatment of periodontal infection given through the intrapocket. It engages with the bacterial cell membrane in order to diminish or potentially eradicate the bacterial population. Nevertheless, current research examining the antibacterial efficacy of doxycycline against oral biofilms remains limited. However, it is important to note that the current *in vitro* investigation demonstrated a maximum reduction of 1 log10 in bacterial counts within the biofilm. This highlights the limitation of antimicrobial agents in eradicating a pre-existing intricate biofilm. Hence, it is advisable to prescribe antimicrobials alongside mechanical biofilm disruption, implying that mechanical biofilm elimination remains the preferred approach in the treatment of periodontitis.[84]

4. CONCLUSIONS

In summary, the current work has demonstrated that the formulation of DOX into MPs loaded in situ hydrogel system for intrapocket delivery was effective in increasing the drug solubility as evidenced by steady-state release *in vitro* and its penetrated amount. Controlled drug delivery systems have the potential to enhance patient adherence and therapeutic effectiveness by enabling accurate regulation of the rate of drug release from the delivery system, thereby eliminating the need for frequent dosing. The previously mentioned drug delivery systems are deemed superior due to their cost-effectiveness, enhanced stability, lack of toxicity, biocompatibility, nonimmunogenicity, and inherent biodegradability. It is feasible to establish a reliable *ex vivo* biofilm model that closely mimics the *in vivo* scenario and facilitates the assessment of diverse antimicrobial agents. This provides evidence that the preparation exhibits potential as a viable option for the treatment of bacterial infections resulting from biofilms of *S. aureus* and *E. coli*. The pH sensitivity of the DOX-MPs *in situ* hydrogel is a crucial factor in determining its antimicrobial activity. However, several further experiments are now needed, including biocompatibility study, nonimmunogenicity test, and mechanical stability test. Additionally, subsequent *in vivo* assessments utilizing an appropriate animal model are necessary to explore the viability of employing it in clinical contexts for combating periodontal bacterial infections.

AUTHOR INFORMATION

Corresponding Author

Karima Qurnia Mansjur − *Department of Orthodontic, Faculty of Dentistry, Hasanuddin University, Makassar 90245, Indonesia;* orcid.org/0000-0001-9132-1229; Email: karimaqurniamansjur@unhas.ac.id

Authors

Ardiyah Nurul Fitri Marzaman − *Faculty of Pharmacy, Hasanuddin University, Makassar 90245, Indonesia*

Ulfah Mahfufah − *Faculty of Pharmacy, Hasanuddin University, Makassar 90245, Indonesia*

Nurul Fauziah − *Faculty of Pharmacy, Hasanuddin University, Makassar 90245, Indonesia*

Fadhlil Ulum Ar Rahman − *Department of Oral Maxillofacial Radiology, Faculty of Dentistry, Hasanuddin University, Makassar 90245, Indonesia*

Nasyrah Hidayati − *Department of Orthodontic, Faculty of Dentistry, Hasanuddin University, Makassar 90245, Indonesia*

Rafikah Hasyim − *Department of Oral Biology, Faculty of Dentistry, Hasanuddin University, Makassar 90245, Indonesia;* orcid.org/0000-0002-2715-0098

Dian Setiawati − *Department of Periodontology, Faculty of Dentistry, Hasanuddin University, Makassar 90245, Indonesia*

Syaiful Choiri − *Faculty of Mathematics and Natural Sciences, Sebelas Maret University, Surakarta 57126, Indonesia;* orcid.org/0000-0001-7750-6008

Nur Aisyah Nuzulia − *Faculty of Mathematics and Natural Sciences, Institute Pertanian Bogor, Bogor 16680, Indonesia*

Aqilah Fidya Madani − *Faculty of Pharmacy, Hasanuddin University, Makassar 90245, Indonesia*

Maria Mir − *Department of Pharmacy, Iqra University, Islamabad Campus 44000, Pakistan*

Andi Dian Permana − *Faculty of Pharmacy, Hasanuddin University, Makassar 90245, Indonesia;* orcid.org/0000-0003-2168-1688

Complete contact information is available at: https://pubs.acs.org/10.1021/acsomega.4c08967

Author Contributions

The manuscript was written through the contribution of all authors. All authors have approved the final version of the manuscript.

Funding

This work was supported by Penelitian Fundamental Kolaboratif No. 00323/UN.4.22/PT.01.03/2023.

Notes

The authors declare no competing financial interest.

ACKNOWLEDGMENTS

This work was supported by Penelitian Fundamental Kolaboratif, Hasanuddin University, Makassar Indonesia.

REFERENCES

(1) Tonetti, M. S.; Greenwell, H.; Kornman, K. S. Staging and Grading of Periodontitis: Framework and Proposal of a New Classification and Case Definition. *J. Periodontol.* **2018**, *89* (S1), S159−S172, DOI: 10.1002/JPER.18-0006.

(2) Bascones-Martinez, A.; Matesanz-Perez, P.; Escribano-Bermejo, M.; Gonzalez-Moles, M. A.; Bascones-Ilundain, J.; Meurman, J. H. Periodontal disease and diabetes-Review of the Literature. *Med. Oral Patol. Oral Cir. Bucal* **2009**, *16* (6), e722−e729.

(3) Vos, T.; Abajobir, A. A.; Abate, K. H.; Abbafati, C.; Abbas, K. M.; Abd-Allah, F.; Abdulkader, R. S.; Abdulle, A. M.; Abebo, T. A.; Abera, S. F.; Aboyans, V.; Abu-Raddad, L. J.; Ackerman, I. N.; Adamu, A. A.; Adetokunboh, O.; Afarideh, M.; Afshin, A.; Agarwal, S. K.; Aggarwal, R.; Agrawal, A.; Agrawal, S.; Ahmadieh, H.; Ahmed, M. B.; Aichour, M. T. E.; Aichour, A. N.; Aichour, I.; Aiyar, S.; Akinyemi, R. O.; Akseer, N.; Al Lami, F. H.; Alahdab, F.; Al-Aly, Z.; Alam, K.; Alam, N.; Alam, T.; Alasfoor, D.; Alene, K. A.; Ali, R.; Alizadeh-Navaei, R.; Alkerwi, A.; Alla, F.; Allebeck, P.; Allen, C.; Al-Maskari, F.; Al-Raddadi, R.; Alsharif, U.; Alsowaidi, S.; Altirkawi, K. A.; Amare, A. T.; Amini, E.; Ammar, W.; Amoako, Y. A.; Andersen, H. H.; Antonio, C. A. T.; Anwari, P.; Ärnlöv, J.; Artaman, A.; Aryal, K. K.; Asayesh, H.; Asgedom, S. W.; Assadi, R.; Atey, T. M.; Atnafu, N. T.; Atre, S. R.; Avila-Burgos, L.; Avokphako, E. F. G. A.; Awasthi, A.; Bacha, U.; Badawi, A.; Balakrishnan, K.; Banerjee, A.; Bannick, M. S.; Barac, A.; Barber, R. M.; Barker-Collo, S. L.; Bärnighausen, T.; Barquera, S.; Barregard, L.; Barrero, L. H.; Basu, S.; Battista, B.; Battle, K. E.; Baune, B. T.; Bazargan-Hejazi, S.; Beardsley, J.; Bedi, N.; Beghi, E.; Béjot, Y.; Bekele, B. B.; Bell, M. L.; Bennett, D. A.; Bensenor, I. M.; Benson, J.; Berhane, A.; Berhe, D. F.; Bernabé, E.; Betsu, B. D.;

Beuran, M.; Beyene, A. S.; Bhala, N.; Bhansali, A.; Bhatt, S.; Bhutta, Z. A.; Biadgilign, S.; Bicer, B. K.; Bienhoff, K.; Bikbov, B.; Birungi, C.; Biryukov, S.; Bisanzio, D.; Bizuayehu, H. M.; Boneya, D. J.; Boufous, S.; Bourne, R. R. A.; Brazinova, A.; Brugha, T. S.; Buchbinder, R.; Bulto, L. N. B.; Bumgarner, B. R.; Butt, Z. A.; Cahuana-Hurtado, L.; Cameron, E.; Car, M.; Carabin, H.; Carapetis, J. R.; Cárdenas, R.; Carpenter, D. O.; Carrero, J. J.; Carter, A.; Carvalho, F.; Casey, D. C.; Caso, V.; Castañeda-Orjuela, C. A.; Castle, C. D.; Catalá-López, F.; Chang, H.-Y.; Chang, J.-C.; Charlson, F. J.; Chen, H.; Chibalabala, M.; Chibueze, C. E.; Chisumpa, V. H.; Chitheer, A. A.; Christopher, D. J.; Ciobanu, L. G.; Cirillo, M.; Colombara, D.; Cooper, C.; Cortesi, P. A.; Criqui, M. H.; Crump, J. A.; Dadi, A. F.; Dalal, K.; Dandona, L.; Dandona, R.; das Neves, J.; Davitoiu, D. V.; de Courten, B.; De Leo, D. De.; Defo, B. K.; Degenhardt, L.; Deiparine, S.; Dellavalle, R. P.; Deribe, K.; Des Jarlais, D. C.; Dey, S.; Dharmaratne, S. D.; Dhillon, P. K.; Dicker, D.; Ding, E. L.; Djalalinia, S.; Do, H. P.; Dorsey, E. R.; dos Santos, K. P. B.; Douwes-Schultz, D.; Doyle, K. E.; Driscoll, T. R.; Dubey, M.; Duncan, B. B.; El-Khatib, Z. Z.; Ellerstrand, J.; Enayati, A.; Endries, A. Y.; Ermakov, S. P.; Erskine, H. E.; Eshrati, B.; Eskandarieh, S.; Esteghamati, A.; Estep, K.; Fanuel, F. B. B.; Farinha, C. S. E. S.; Faro, A.; Farzadfar, F.; Fazeli, M. S.; Feigin, V. L.; Fereshtehnejad, S.-M.; Fernandes, J. C.; Ferrari, A. J.; Feyissa, T. R.; Filip, I.; Fischer, F.; Fitzmaurice, C.; Flaxman, A. D.; Flor, L. S.; Foigt, N.; Foreman, K. J.; Franklin, R. C.; Fullman, N.; Fürst, T.; Furtado, J. M.; Futran, N. D.; Gakidou, E.; Ganji, M.; Garcia-Basteiro, A. L.; Gebre, T.; Gebrehiwot, T. T.; Geleto, A.; Gemechu, B. L.; Gesesew, H. A.; Gething, P. W.; Ghajar, A.; Gibney, K. B.; Gill, P. S.; Gillum, R. F.; Ginawi, I. A. M.; Giref, A. Z.; Gishu, M. D.; Giussani, G.; Godwin, W. W.; Gold, A. L.; Goldberg, E. M.; Gona, P. N.; Goodridge, A.; Gopalani, S. V.; Goto, A.; Goulart, A. C.; Griswold, M.; Gugnani, H. C.; Gupta, R.; Gupta, R.; Gupta, T.; Gupta, V.; Hafezi-Nejad, N.; Hailu, G. B.; Hailu, A. D.; Hamadeh, R. R.; Hamidi, S.; Handal, A. J.; Hankey, G. J.; Hanson, S. W.; Hao, Y.; Harb, H. L.; Hareri, H. A.; Haro, J. M.; Harvey, J.; Hassanvand, M. S.; Havmoeller, R.; Hawley, C.; Hay, S. I.; Hay, R. J.; Henry, N. J.; Heredia-Pi, I. B.; Hernandez, J. M.; Heydarpour, P.; Hoek, H. W.; Hoffman, H. J.; Horita, N.; Hosgood, H. D.; Hostiuc, S.; Hotez, P. J.; Hoy, D. G.; Htet, A. S.; Hu, G.; Huang, H.; Huynh, C.; Iburg, K. M.; Igumbor, E. U.; Ikeda, C.; Irvine, C. M. S.; Jacobsen, K. H.; Jahanmehr, N.; Jakovljevic, M. B.; Jassal, S. K.; Javanbakht, M.; Jayaraman, S. P.; Jeemon, P.; Jensen, P. N.; Jha, V.; Jiang, G.; John, D.; Johnson, S. C.; Johnson, C. O.; Jonas, J. B.; Jürisson, M.; Kabir, Z.; Kadel, R.; Kahsay, A.; Kamal, R.; Kan, H.; Karam, N. E.; Karch, A.; Karema, C. K.; Kasaeian, A.; Kassa, G. M.; Kassaw, N. A.; Kassebaum, N. J.; Kastor, A.; Katikireddi, S. V.; Kaul, A.; Kawakami, N.; Keiyoro, P. N.; Kengne, A. P.; Keren, A.; Khader, Y. S.; Khalil, I. A.; Khan, E. A.; Khang, Y.-H.; Khosravi, A.; Khubchandani, J.; Kiadaliri, A. A.; Kieling, C.; Kim, Y. J.; Kim, D.; Kim, P.; Kimokoti, R. W.; Kinfu, Y.; Kisa, A.; Kissimova-Skarbek, K. A.; Kivimaki, M.; Knudsen, A. K.; Kokubo, Y.; Kolte, D.; Kopec, J. A.; Kosen, S.; Koul, P. A.; Koyanagi, A.; Kravchenko, M.; Krishnaswami, S.; Krohn, K. J.; Kumar, G. A.; Kumar, P.; Kumar, S.; Kyu, H. H.; Lal, D. K.; Lalloo, R.; Lambert, N.; Lan, Q.; Larsson, A.; Lavados, P. M.; Leasher, J. L.; Lee, P. H.; Lee, J.-T.; Leigh, J.; Leshargie, C. T.; Leung, J.; Leung, R.; Levi, M.; Li, Y.; Li, Y.; Li Kappe, D.; Liang, X.; Liben, M. L.; Lim, S. S.; Linn, S.; Liu, P. Y.; Liu, A.; Liu, S.; Liu, Y.; Lodha, R.; Logroscino, G.; London, S. J.; Looker, K. J.; Lopez, A. D.; Lorkowski, S.; Lotufo, P. A.; Low, N.; Lozano, R.; Lucas, T. C. D.; Macarayan, E. R. K.; Magdy Abd El Razek, H.; Magdy Abd El Razek, M.; Mahdavi, M.; Majdan, M.; Majdzadeh, R.; Majeed, A.; Malekzadeh, R.; Malhotra, R.; Malta, D. C.; Mamun, A. A.; Manguerra, H.; Manhertz, T.; Mantilla, A.; Mantovani, L. G.; Mapoma, C. C.; Marczak, L. B.; Martinez-Raga, J.; Martins-Melo, F. R.; Martopullo, I.; März, W.; Mathur, M. R.; Mazidi, M.; McAlinden, C.; McGaughey, M.; McGrath, J. J.; McKee, M.; McNellan, C.; Mehata, S.; Mehndiratta, M. M.; Mekonnen, T. C.; Memiah, P.; Memish, Z. A.; Mendoza, W.; Mengistie, M. A.; Mengistu, D. T.; Mensah, G. A.; Meretoja, T. J.; Meretoja, A.; Mezgebe, H. B.; Micha, R.; Millear, A.; Miller, T. R.; Mills, E. J.; Mirarefin, M.; Mirrakhimov, E. M.; Misganaw, A.; Mishra, S. R.; Mitchell, P. B.; Mohammad, K. A.; Mohammadi, A.; Mohammed, K. E.; Mohammed, S.; Mohanty, S. K.; Mokdad, A. H.; Mollenkopf, S. K.; Monasta, L.; Montico, M.; Moradi-Lakeh, M.; Moraga, P.; Mori, R.; Morozoff, C.; Morrison, S. D.; Moses, M.; Mountjoy-Venning, C.; Mruts, K. B.; Mueller, U. O.; Muller, K.; Murdoch, M. E.; Murthy, G. V. S.; Musa, K. I.; Nachega, J. B.; Nagel, G.; Naghavi, M.; Naheed, A.; Naidoo, K. S.; Naldi, L.; Nangia, V.; Natarajan, G.; Negasa, D. E.; Negoi, R. I.; Negoi, I.; Newton, C. R.; Ngunjiri, J. W.; Nguyen, T. H.; Nguyen, Q. Le.; Nguyen, C. T.; Nguyen, G.; Nguyen, M.; Nichols, E.; Ningrum, D. N. A.; Nolte, S.; Nong, V. M.; Norrving, B.; Noubiap, J. J. N.; O'Donnell, M. J.; Ogbo, F. A.; Oh, I.-H.; Okoro, A.; Oladimeji, O.; Olagunju, T. O.; Olagunju, A. T.; Olsen, H. E.; Olusanya, B. O.; Olusanya, J. O.; Ong, K.; Opio, J. N.; Oren, E.; Ortiz, A.; Osgood-Zimmerman, A.; Osman, M.; Owolabi, M. O.; PA, M.; Pacella, R. E.; Pana, A.; Panda, B. K.; Papachristou, C.; Park, E.-K.; Parry, C. D.; Parsaeian, M.; Patten, S. B.; Patton, G. C.; Paulson, K.; Pearce, N.; Pereira, D. M.; Perico, N.; Pesudovs, K.; Peterson, C. B.; Petzold, M.; Phillips, M. R.; Pigott, D. M.; Pillay, J. D.; Pinho, C.; Plass, D.; Pletcher, M. A.; Popova, S.; Poulton, R. G.; Pourmalek, F.; Prabhakaran, D.; Prasad, N. M.; Prasad, N.; Purcell, C.; Qorbani, M.; Quansah, R.; Quintanilla, B. P. A.; Rabiee, R. H. S.; Radfar, A.; Rafay, A.; Rahimi, K.; Rahimi-Movaghar, A.; Rahimi-Movaghar, V.; Rahman, M. H. U.; Rahman, M.; Rai, R. K.; Rajsic, S.; Ram, U.; Ranabhat, C. L.; Rankin, Z.; Rao, P. C.; Rao, P. V.; Rawaf, S.; Ray, S. E.; Reiner, R. C.; Reinig, N.; Reitsma, M. B.; Remuzzi, G.; Renzaho, A. M. N.; Resnikoff, S.; Rezaei, S.; Ribeiro, A. L.; Ronfani, L.; Roshandel, G.; Roth, G. A.; Roy, A.; Rubagotti, E.; Ruhago, G. M.; Saadat, S.; Sadat, N.; Safdarian, M.; Safi, S.; Safiri, S.; Sagar, R.; Sahathevan, R.; Salama, J.; Saleem, H. O. B.; Salomon, J. A.; Salvi, S. S.; Samy, A. M.; Sanabria, J. R.; Santomauro, D.; Santos, I. S.; Santos, J. V.; Santric Milicevic, M. M.; Sartorius, B.; Satpathy, M.; Sawhney, M.; Saxena, S.; Schmidt, M. I.; Schneider, I. J. C.; Schöttker, B.; Schwebel, D. C.; Schwendicke, F.; Seedat, S.; Sepanlou, S. G.; Servan-Mori, E. E.; Setegn, T.; Shackelford, K. A.; Shaheen, A.; Shaikh, M. A.; Shamsipour, M.; Shariful Islam, S. M.; Sharma, J.; Sharma, R.; She, J.; Shi, P.; Shields, C.; Shifa, G. T.; Shigematsu, M.; Shinohara, Y.; Shiri, R.; Shirkoohi, R.; Shirude, S.; Shishani, K.; Shrime, M. G.; Sibai, A. M.; Sigfusdottir, I. D.; Silva, D. A. S.; Silva, J. P.; Silveira, D. G. A.; Singh, J. A.; Singh, N. P.; Sinha, D. N.; Skiadaresi, E.; Skirbekk, V.; Slepak, E. L.; Sligar, A.; Smith, D. L.; Smith, M.; Sobaih, B. H. A.; Sobngwi, E.; Sorensen, R. J. D.; Sousa, T. C. M.; Sposato, L. A.; Sreeramareddy, C. T.; Srinivasan, V.; Stanaway, J. D.; Stathopoulou, V.; Steel, N.; Stein, M. B.; Stein, D. J.; Steiner, T. J.; Steiner, C.; Steinke, S.; Stokes, M. A.; Stovner, L. J.; Strub, B.; Subart, M.; Sufiyan, M. B.; Sunguya, B. F.; Sur, P. J.; Swaminathan, S.; Sykes, B. L.; Sylte, D. O.; Tabarés-Seisdedos, R.; Taffere, G. R.; Takala, J. S.; Tandon, N.; Tavakkoli, M.; Taveira, N.; Taylor, H. R.; Tehrani-Banihashemi, A.; Tekelab, T.; Terkawi, A. S.; Tesfaye, D. J.; Tesssema, B.; Thamsuwan, O.; Thomas, K. E.; Thrift, A. G.; Tiruye, T. Y.; Tobe-Gai, R.; Tollanes, M. C.; Tonelli, M.; Topor-Madry, R.; Tortajada, M.; Touvier, M.; Tran, B. X.; Tripathi, S.; Troeger, C.; Truelsen, T.; Tsoi, D.; Tuem, K. B.; Tuzcu, E. M.; Tyrovolas, S.; Ukwaja, K. N.; Undurraga, E. A.; Uneke, C. J.; Updike, R.; Uthman, O. A.; Uzochukwu, B. S. C.; van Boven, J. F. M.; Varughese, S.; Vasankari, T.; Venkatesh, S.; Venketasubramanian, N.; Vidavalur, R.; Violante, F. S.; Vladimirov, S. K.; Vlassov, V. V.; Vollset, S. E.; Wadilo, F.; Wakayo, T.; Wang, Y.-P.; Weaver, M.; Weichenthal, S.; Weiderpass, E.; Weintraub, R. G.; Werdecker, A.; Westerman, R.; Whiteford, H. A.; Wijeratne, T.; Wiysonge, C. S.; Wolfe, C. D. A.; Woodbrook, R.; Woolf, A. D.; Workicho, A.; Xavier, D.; Xu, G.; Yadgir, S.; Yaghoubi, M.; Yakob, B.; Yan, L. L.; Yano, Y.; Ye, P.; Yimam, H. H.; Yip, P.; Yonemoto, N.; Yoon, S.-J.; Yotebieng, M.; Younis, M. Z.; Zaidi, Z.; Zaki, M. E. S.; Zegeye, E. A.; Zenebe, Z. M.; Zhang, X.; Zhou, M.; Zipkin, B.; Zodpey, S.; Zuhlke, L. J.; Murray, C. J. L. Global, Regional, and National Incidence, Prevalence, and Years Lived with Disability for 328 Diseases and Injuries for 195 Countries, 1990−2016: A Systematic Analysis for the Global Burden of Disease Study 2016. *Lancet* **2017**, *390* (10100), 1211−1259.

https://doi.org/10.1021/acsomega.4c08967
ACS Omega 2025, 10, 5668−5685

(4) Eke, P. I.; Dye, B. A.; Wei, L.; Thornton-Evans, G. O.; Genco, R. J. Prevalence of Periodontitis in Adults in the United States: 2009 and 2010. *J. Dent Res.* **2012**, *91* (10), 914−920.
(5) Nazir, M. A. Prevalence of Periodontal Disease, Its Association with Systemic Diseases and Prevention. *Int. J. Health Sci.* **2017**, *11* (2), 72−80.
(6) Könönen, E.; Gursoy, M.; Gursoy, U. Periodontitis: A Multifaceted Disease of Tooth-Supporting Tissues. *J. Clin. Med.* **2019**, *8* (8), 1135.
(7) Flemming, H.-C.; Wingender, J. The Biofilm Matrix. *Nat. Rev. Microbiol.* **2010**, *8* (9), 623−633.
(8) Merkel, A.; Chen, Y.; Villani, C.; George, A. GRP78 Promotes the Osteogenic and Angiogenic Response in Periodontal Ligament Stem Cells. *Eur. Cell Mater.* **2023**, *45*, 14−30.
(9) Li, J.; Kou, N.; Shi, X.; Kong, L.; Chen, W.; Yang, X.; Zhao, Y.; Zhao, J.; Wang, F. Inhibition of Soluble Epoxide Hydrolase Reverses Bone Loss in Periodontitis by Upregulating EMCN and Inhibiting Osteoclasts. *Stem Cell Res. Ther.* **2024**, *15* (1), 451.
(10) Sun, L.; Du, X.; Kuang, H.; Sun, H.; Luo, W.; Yang, C. Stem Cell-Based Therapy in Periodontal Regeneration: A Systematic Review and Meta-Analysis of Clinical Studies. *BMC Oral Health* **2023**, *23* (1), 492.
(11) Wen, S.; Zheng, X.; Yin, W.; Liu, Y.; Wang, R.; Zhao, Y.; Liu, Z.; Li, C.; Zeng, J.; Rong, M. Dental Stem Cell Dynamics in Periodontal Ligament Regeneration: From Mechanism to Application. *Stem Cell Res. Ther.* **2024**, *15* (1), 389.
(12) Quirynen, M.; Teughels, W.; De Soete, M.; Van Steenberghe, D. Topical Antiseptics and Antibiotics in the Initial Therapy of Chronic Adult Periodontitis: Microbiological Aspects. *Periodontology 2000* **2002**, *28* (1), 72−90.
(13) Könönen, E.; Gursoy, M.; Gursoy, U. Periodontitis: A Multifaceted Disease of Tooth-Supporting Tissues. *J. Clin. Med.* **2019**, *8* (8), 1135.
(14) Parsons, R.; Summers, S. The Role of Case Studies in Effective Data Sharing, Reuse and Impact. *IASSIST Q.* **2017**, *40* (3), 14.
(15) Adhirajan, N.; Shanmugasundaram, N.; Shanmuganathan, S.; Babu, M. Collagen-Based Wound Dressing for Doxycycline Delivery: In-Vivo Evaluation in an Infected Excisional Wound Model in Rats. *J. Pharm. Pharmacol.* **2009**, *61* (12), 1617−1623.
(16) Sader, H. S.; Jones, R. N.; Silva, J. B. Skin and Soft Tissue Infections in Latin American Medical Centers: Four-Year Assessment of the Pathogen Frequency and Antimicrobial Susceptibility Patterns. *Diagn. Microbiol. Infect. Dis.* **2002**, *44* (3), 281−288.
(17) Lai, C.-C.; Chen, C.-C.; Huang, H.-L.; Chuang, Y.-C.; Tang, H.-J. The Role of Doxycycline in the Therapy of Multidrug-Resistant *E. Coli* − an in Vitro Study. *Sci. Rep.* **2016**, *6* (1), No. 31964.
(18) Abasaheb Borse, V.; Gangude, A. B.; Deore, A. B. Formulation and Evaluation of Antibacterial Topical Gel of Doxycycline Hyclate, Neem Oil and Tea Tree Oil. *Indian J. Pharm. Educ. Res.* **2019**, *54* (1), 206−212.
(19) Allen, T. M.; Cullis, P. R. Drug Delivery Systems: Entering the Mainstream. *Science* **2004**, *303* (5665), 1818−1822.
(20) Galgut, P. N. The Relevance of PH to Gingivitis and Periodontitis. *J. Int. Acad. Periodontol.* **2001**, *3* (3), 61−67.
(21) Liao, Z. X.; et al. 21. pH-sensitive chitosan-based nanoparticles for protein drug delivery: oral approaches: Original research article: a novel pH-sensitive hydrogel composed of carboxymethyl chitosan and alginate cross-linked by genipin for protein drug delivery, 2004. *J. Controlled Release* **2014**, *190*, 68−70, DOI: 10.1016/j.jconrel.2014.07.033.
(22) Haffajee, A. D.; Socransky, S. S.; Gunsolley, J. C. Systemic Anti-Infective Periodontal Therapy. A Systematic Review. *Ann. Periodontol.* **2003**, *8* (1), 115−181.
(23) Kapoor, A.; Malhotra, R.; Grover, V.; Grover, D. Systemic Antibiotic Therapy in Periodontics. *Dent Res. J.* **2012**, *9* (5), 505.
(24) López, N. J.; Quintero, A.; Casanova, P. A.; Ibieta, C. I.; Baelum, V.; López, R. Effects of Periodontal Therapy on Systemic Markers of Inflammation in Patients With Metabolic Syndrome: A Controlled Clinical Trial. *J. Periodontol.* **2012**, *83* (3), 267−278.
(25) Kerry, G. Tetracycline-Loaded Fibers as Adjunctive Treatment In Periodontal Disease. *J. Am. Dent. Assoc.* **1994**, *125* (9), 1199−1203.
(26) Griffiths, G. S.; Smart, G. J.; Bulman, J. S.; Weiss, G.; Shrowder, J.; Newman, H. N. Comparison of Clinical Outcomes Following Treatment of Chronic Adult Periodontitis with Subgingival Scaling or Subgingival Scaling plus Metronidazole Gel. *J. Clin. Periodontol.* **2000**, *27* (12), 910−917.
(27) Isola, G.; Polizzi, A.; Santonocito, S.; Dalessandri, D.; Migliorati, M.; Indelicato, F. New Frontiers on Adjuvants Drug Strategies and Treatments in Periodontitis. *Sci. Pharm.* **2021**, *89* (4), 46.
(28) Rabea, E. I.; Badawy, M. E.-T.; Stevens, C. V.; Smagghe, G.; Steurbaut, W. Chitosan as Antimicrobial Agent: Applications and Mode of Action. *Biomacromolecules* **2003**, *4* (6), 1457−1465.
(29) Mansjur, K. Q.; Attaya, N. S.; Erwansyah, E.; Pawinru, A. S.; Nasir, M. The Effect of Coating Chitosan from Cuttlefish Bone (Sepia Sp.) on the Surface of Orthodontic Mini-Screw. *OpenNano* **2024**, *20*, 100217.
(30) Han, C.; Romero, N.; Fischer, S.; Dookran, J.; Berger, A.; Doiron, A. L. Recent Developments in the Use of Nanoparticles for Treatment of Biofilms. *Nanotechnol. Rev.* **2017**, *6* (5), 383−404.
(31) Anderson, J. M.; Shive, M. S. Biodegradation and Biocompatibility of PLA and PLGA Microspheres. *Adv. Drug Delivery Rev.* **2012**, *64*, 72−82.
(32) Chang, P.; Chung, M. C.; Lei, C.; Chong, L. Y.; Wang, C. H. Biocompatibility of PDGF-simvastatin Double-walled PLGA (PDLLA) Microspheres for Dentoalveolar Regeneration: A Preliminary Study. *J. Biomed. Mater. Res., Part A* **2012**, *100A* (11), 2970−2978.
(33) Lu, L.; Peter, S. J.; D Lyman, M.; Lai, H.-L.; Leite, S. M.; Tamada, J. A.; Uyama, S.; Vacanti, J. P.; Robert, L.; Mikos, A. G. In Vitro and in Vivo Degradation of Porous Poly(Dl-Lactic-Co-Glycolic Acid) Foams. *Biomaterials* **2000**, *21* (18), 1837−1845.
(34) Mudjahid, M.; Nainu, F.; Utami, R. N.; Sam, A.; Marzaman, A. N. F.; Roska, T. P.; Asri, R. M.; Himawan, A.; Donnelly, R. F.; Permana, A. D. Enhancement in Site-Specific Delivery of Chloramphenicol Using Bacterially Sensitive Microparticle Loaded Into Dissolving Microneedle: Potential For Enhanced Effectiveness Treatment of Cellulitis. *ACS Appl. Mater. Interfaces* **2022**, *14* (51), 56560−56577.
(35) Botrel, D. A.; Rodrigues, I. C.; de Souza, H. J.; de Barros Fernandes, R. V. Application of inulin in thin-layer drying process of araticum (Annona crassiflora) pulp. *LWT - Food Sci. Technol.* **2016**, *69*, 32−39.
(36) Xiong, M.; Li, Y.; Bao, Y.; Yang, X.; Hu, B.; Wang, J. Bacteria-Responsive Multifunctional Nanogel for Targeted Antibiotic Delivery. *Adv. Mater.* **2012**, *24* (46), 6175−6180.
(37) Maharani, S. N. K.; Hidayat, Muh. T.; Ramadhany, I. D.; Khairani, N. I.; Rahman, N. A.; Permana, A. D. Application of Validated UV−Vis Spectrophotometry-Colorimetric Methods for Specific Quantification of Deferiprone in the Development of Iron-Responsive Nanoparticle Loaded into Dissolving Microneedle. *Microchim. Acta* **2024**, *191* (10), 587.
(38) Febrianti, N. Q.; Tunggeng, M. G. R.; Ramadhany, I. D.; Asri, R. M.; Djabir, Y. Y.; Permana, A. D. Validation of UV−Vis Spectrophotometric and Colorimetric Methods to Quantify Methotrexate in Plasma and Rat Skin Tissue: Application to in Vitro Release, Ex Vivo and in Vivo Studies from Dissolving Microarray Patch Loaded PH-Sensitive Nanoparticle. *Spectrochim. Acta, Part A* **2024**, *315*, No. 124258.
(39) Hamdan, M. F.; Ramadhani, N. N.; Aziz, A. Y. R.; Sahra, M.; Agrabudi, A. I.; Permana, A. D. Development and Validation of UV−Vis Spectrophotometry-Colorimetric Method for the Specific Quantification of Rivastigmine Tartrate from Separable Effervescent Microneedles: Ex Vivo and in Vivo Applications in Complex Biological Matrices. *J. Mol. Struct.* **2024**, *1303*, No. 137589.
(40) Permana, A. D.; McCrudden, M. T. C.; Donnelly, R. F. Enhanced Intradermal Delivery of Nanosuspensions of Antifilariasis

https://doi.org/10.1021/acsomega.4c08967
ACS Omega 2025, 10, 5668−5685

Drugs Using Dissolving Microneedles: A Proof of Concept Study. *Pharmaceutics* **2019**, *11* (7), 346.
(41) Permana, A. D.; Tekko, I. A.; McCrudden, M. T. C.; Anjani, Q. K.; Ramadon, D.; McCarthy, H. O.; Donnelly, R. F. Solid Lipid Nanoparticle-Based Dissolving Microneedles: A Promising Intradermal Lymph Targeting Drug Delivery System with Potential for Enhanced Treatment of Lymphatic Filariasis. *J. Controlled Release* **2019**, *316*, 34−52.
(42) Permana, A. D.; Anjani, Q. K.; Sartini; Utomo, E.; Volpe-Zanutto, F.; Paredes, A. J.; Evary, Y. M.; Mardikasari, S. A.; Pratama, M. R.; Tuany, I. N.; Donnelly, R. F. Selective Delivery of Silver Nanoparticles for Improved Treatment of Biofilm Skin Infection Using Bacteria-Responsive Microparticles Loaded into Dissolving Microneedles. *Mater. Sci. Eng.: C* **2021**, *120*, No. 111786.
(43) Permana, A. D.; Mir, M.; Utomo, E.; Donnelly, R. F. Bacterially Sensitive Nanoparticle-Based Dissolving Microneedles of Doxycycline for Enhanced Treatment of Bacterial Biofilm Skin Infection: A Proof of Concept Study. *Int. J. Pharm. X* **2020**, *2*, No. 100047.
(44) Khattab, A.; Marzok, S.; Ibrahim, M. Development of Optimized Mucoadhesive Thermosensitive Pluronic Based in Situ Gel for Controlled Delivery of Latanoprost: Antiglaucoma Efficacy and Stability Approaches. *J. Drug Delivery Sci. Technol.* **2019**, *53*, No. 101134.
(45) Nurul Fitri Marzaman, A.; Sartini; Mudjahid, M.; Puspita Roska, T.; Sam, A.; Permana, A. D. Development of Chloramphenicol Whey Protein-Based Microparticles Incorporated into Thermoresponsive in Situ Hydrogels for Improved Wound Healing Treatment. *Int. J. Pharm.* **2022**, *628*, No. 122323.
(46) Walker, C.; Sedlacek, M. J. An *in Vitro* Biofilm Model of Subgingival Plaque. *Oral Microbiol. Immunol.* **2007**, *22* (3), 152−161.
(47) Din, F.; Mustapha, O.; Kim, D. W.; Rashid, R.; Park, J. H.; Choi, J. Y.; Ku, S. K.; Yong, C. S.; Kim, J. O.; Choi, H.-G. Novel Dual-Reverse Thermosensitive Solid Lipid Nanoparticle-Loaded Hydrogel for Rectal Administration of Flurbiprofen with Improved Bioavailability and Reduced Initial Burst Effect. *Eur. J. Pharm. Biopharm.* **2015**, *94*, 64−72.
(48) Chen, J.; Zhou, R.; Li, L.; Li, B.; Zhang, X.; Su, J. Mechanical, Rheological and Release Behaviors of a Poloxamer 407/ Poloxamer 188/Carbopol 940 Thermosensitive Composite Hydrogel. *Molecules* **2013**, *18* (10), 12415−12425.
(49) Qiu, Y.; Man, R. C. H.; Liao, Q.; Kung, K. L. K.; Chow, M. Y. T.; Lam, J. K. W. Effective MRNA Pulmonary Delivery by Dry Powder Formulation of PEGylated Synthetic KL4 Peptide. *J. Controlled Release* **2019**, *314*, 102−115.
(50) Alqahtani, S.; Simon, L.; Astete, C. E.; Alayoubi, A.; Sylvester, P. W.; Nazzal, S.; Shen, Y.; Xu, Z.; Kaddoumi, A.; Sabliov, C. M. Cellular Uptake, Antioxidant and Antiproliferative Activity of Entrapped α-Tocopherol and γ-Tocotrienol in Poly (Lactic-Co-Glycolic) Acid (PLGA) and Chitosan Covered PLGA Nanoparticles (PLGA-Chi). *J. Colloid Interface Sci.* **2015**, *445*, 243−251.
(51) Hill, L. E.; Taylor, T. M.; Gomes, C. Antimicrobial Efficacy of Poly (DL-lactide-co-glycolide) (PLGA) Nanoparticles with Entrapped Cinnamon Bark Extract against *Listeria Monocytogenes* and *Salmonella Typhimurium*. *J. Food Sci.* **2013**, *78* (4), N626−N632, DOI: 10.1111/1750-3841.12069.
(52) Huang, W. F.; Tsui, C. P.; Tang, C. Y.; Yang, M.; Gu, L. Surface Charge Switchable and PH-Responsive Chitosan/Polymer Core-Shell Composite Nanoparticles for Drug Delivery Application. *Composites, Part B* **2017**, *121*, 83−91.
(53) Fialho e Moraes, A. R.; Pola, C. C.; Bilck, A. P.; Yamashita, F.; Tronto, J.; Medeiros, E. A. A.; Soares, N. de F. F. Starch, Cellulose Acetate and Polyester Biodegradable Sheets: Effect of Composition and Processing Conditions. *Mater. Sci. Eng.: C* **2017**, *78*, 932−941.
(54) Li, Y.; Kong, D.; Wu, H. Analysis and Evaluation of Essential Oil Components of Cinnamon Barks Using GC−MS and FTIR Spectroscopy. *Ind. Crops Prod.* **2013**, *41*, 269−278.
(55) Ignjatović, N.; Wu, V.; Ajduković, Z.; Mihajilov-Krstev, T.; Uskoković, V.; Uskoković, D. Chitosan-PLGA Polymer Blends as Coatings for Hydroxyapatite Nanoparticles and Their Effect on Antimicrobial Properties, Osteoconductivity and Regeneration of Osseous Tissues. *Mater. Sci. Eng.: C* **2016**, *60*, 357−364.
(56) Yan, D.; Li, Y.; Liu, Y.; Li, N.; Zhang, X.; Yan, C. Antimicrobial Properties of Chitosan and Chitosan Derivatives in the Treatment of Enteric Infections. *Molecules* **2021**, *26* (23), 7136.
(57) Klein, M. P.; Hackenhaar, C. R.; Lorenzoni, A. S. G.; Rodrigues, R. C.; Costa, T. M. H.; Ninow, J. L.; Hertz, P. F. Chitosan Crosslinked with Genipin as Support Matrix for Application in Food Process: Support Characterization and β-d-Galactosidase Immobilization. *Carbohydr. Polym.* **2016**, *137*, 184−190.
(58) Oliveira, D. A.; Angonese, M.; Ferreira, S. R. S.; Gomes, C. L. Nanoencapsulation of Passion Fruit By-Products Extracts for Enhanced Antimicrobial Activity. *Food Bioprod. Process.* **2017**, *104*, 137−146.
(59) Kittur, F. S.; Harish Prashanth, K. V.; Udaya Sankar, K.; Tharanathan, R. N. Characterization of Chitin, Chitosan and Their Carboxymethyl Derivatives by Differential Scanning Calorimetry. *Carbohydr. Polym.* **2002**, *49* (2), 185−193.
(60) Zigoneanu, I. G.; Astete, C. E.; Sabliov, C. M. Nanoparticles with Entrapped α-Tocopherol: Synthesis, Characterization, and Controlled Release. *Nanotechnology* **2008**, *19* (10), No. 105606.
(61) Jain, G. K.; Pathan, S. A.; Akhter, S.; Ahmad, N.; Jain, N.; Talegaonkar, S.; Khar, R. K.; Ahmad, F. J. Mechanistic Study of Hydrolytic Erosion and Drug Release Behaviour of PLGA Nanoparticles: Influence of Chitosan. *Polym. Degrad. Stab.* **2010**, *95* (12), 2360−2366.
(62) Khanal, S.; Adhikari, U.; Rijal, N.; Bhattarai, S.; Sankar, J.; Bhattarai, N. PH-Responsive PLGA Nanoparticle for Controlled Payload Delivery of Diclofenac Sodium. *J. Funct. Biomater.* **2016**, *7* (3), 21.
(63) Fredenberg, S.; Wahlgren, M.; Reslow, M.; Axelsson, A. The Mechanisms of Drug Release in Poly(Lactic-Co-Glycolic Acid)-Based Drug Delivery Systems—A Review. *Int. J. Pharm.* **2011**, *415* (1−2), 34−52.
(64) Permana, A. D.; Tekko, I. A.; McCrudden, M. T. C.; Anjani, Q. K.; Ramadon, D.; McCarthy, H. O.; Donnelly, R. F. Solid Lipid Nanoparticle-Based Dissolving Microneedles: A Promising Intradermal Lymph Targeting Drug Delivery System with Potential for Enhanced Treatment of Lymphatic Filariasis. *J. Controlled Release* **2019**, *316*, 34−52.
(65) Permana, A. D.; Anjani, Q. K.; Sartini; Utomo, E.; Volpe-Zanutto, F.; Paredes, A. J.; Evary, Y. M.; Mardikasari, S. A.; Pratama; Muh, R.; Tuany, I. N.; Donnelly, R. F. Selective Delivery of Silver Nanoparticles for Improved Treatment of Biofilm Skin Infection Using Bacteria-Responsive Microparticles Loaded into Dissolving Microneedles. *Mater. Sci. Eng.: C* **2021**, *120*, No. 111786.
(66) Stevanovic, M.; Uskokovic, D. Poly(Lactide-Co-Glycolide)-Based Micro and Nanoparticles for the Controlled Drug Delivery of Vitamins. *Curr. Nanosci.* **2009**, *5* (1), 1−14.
(67) Arafat, M.; Sarfraz, M.; AbuRuz, S. Development and In Vitro Evaluation of Controlled Release Viagra Containing Poloxamer-188 Using Gastroplus PBPK Modeling Software for In Vivo Predictions and Pharmacokinetic Assessments. *Pharmaceuticals* **2021**, *14* (5), 479.
(68) Danhier, F.; Ansorena, E.; Silva, J. M.; Coco, R.; Le Breton, A.; Préat, V. PLGA-Based Nanoparticles: An Overview of Biomedical Applications. *J. Controlled Release* **2012**, *161* (2), 505−522.
(69) Burt, S. Essential Oils: Their Antibacterial Properties and Potential Applications in Foods—a Review. *Int. J. Food Microbiol.* **2004**, *94* (3), 223−253.
(70) Ravichandran, M.; Hettiarachchy, N. S.; Ganesh, V.; Ricke, S. C.; Singh, S. Enhancement of antimicrobial activities of naturally occurring phenolic compounds by nanoscale delivery against Listeria monocytogenes, Escherichia coli O157: H7 and Salmonella Typhimurium in broth and chicken meat system. *J. Food Saf.* **2011**, *31* (4), 462−471.
(71) Silva, L. M.; Hill, L. E.; Figueiredo, E.; Gomes, C. L. Delivery of Phytochemicals of Tropical Fruit By-Products Using Poly (Dl-Lactide-Co-Glycolide) (PLGA) Nanoparticles: Synthesis, Characterization, and Antimicrobial Activity. *Food Chem.* **2014**, *165*, 362−370.

https://doi.org/10.1021/acsomega.4c08967
ACS Omega 2025, 10, 5668−5685

(72) Pola, C. C.; Moraes, A. R. F.; Medeiros, E. A. A.; Teófilo, R. F.; Soares, N. F. F.; Gomes, C. L. Development and Optimization of PH-Responsive PLGA-Chitosan Nanoparticles for Triggered Release of Antimicrobials. *Food Chem.* **2019**, *295*, 671−679.
(73) Verheul, R. J.; Amidi, M.; van der Wal, S.; van Riet, E.; Jiskoot, W.; Hennink, W. E. Synthesis, Characterization and in Vitro Biological Properties of O-Methyl Free N,N,N-Trimethylated Chitosan. *Biomaterials* **2008**, *29* (27), 3642−3649.
(74) Kong, M.; Chen, X. G.; Xing, K.; Park, H. J. Antimicrobial Properties of Chitosan and Mode of Action: A State of the Art Review. *Int. J. Food Microbiol.* **2010**, *144* (1), 51−63.
(75) Krtalić, I.; Radošević, S.; Hafner, A.; Grassi, M.; Nenadić, M.; Cetina-Čižmek, B.; Filipović-Grčić, J.; Pepić, I.; Lovrić, J. D-Optimal Design in the Development of Rheologically Improved In Situ Forming Ophthalmic Gel. *J. Pharm. Sci.* **2018**, *107* (6), 1562−1571.
(76) Notario-Pérez, F.; Martín-Illana, A.; Cazorla-Luna, R.; Ruiz-Caro, R.; Bedoya, L.-M.; Peña, J.; Veiga, M.-D. Development of Mucoadhesive Vaginal Films Based on HPMC and Zein as Novel Formulations to Prevent Sexual Transmission of HIV. *Int. J. Pharm.* **2019**, *570*, No. 118643.
(77) Notario-Pérez, F.; Martín-Illana, A.; Cazorla-Luna, R.; Ruiz-Caro, R.; Bedoya, L.-M.; Tamayo, A.; Rubio, J.; Veiga, M.-D. Influence of Chitosan Swelling Behaviour on Controlled Release of Tenofovir from Mucoadhesive Vaginal Systems for Prevention of Sexual Transmission of HIV. *Mar. Drugs* **2017**, *15* (2), 50.
(78) Enggi, C. K.; Isa, H. T.; Sulistiawati, S.; Ardika, K. A. R.; Wijaya, S.; Asri, R. M.; Mardikasari, S. A.; Donnelly, R. F.; Permana, A. D. Development of Thermosensitive and Mucoadhesive Gels of Cabotegravir for Enhanced Permeation and Retention Profiles in Vaginal Tissue: A Proof of Concept Study. *Int. J. Pharm.* **2021**, *609*, No. 121182.
(79) Radwan, M. T.; Sin, Ç.; Akkaya, N.; Vahdettin, L. Artificial intelligence-based algorithm for cervical vertebrae maturation stage assessment. *Orthod. Craniofacial Res.* **2023**, *26* (3), 349−355.
(80) Bercea, M.; Constantin, M.; Plugariu, I.-A.; Oana Daraba, M.; Luminita Ichim, D. Thermosensitive Gels of Pullulan and Poloxamer 407 as Potential Injectable Biomaterials. *J. Mol. Liq.* **2022**, *362*, No. 119717.
(81) Aframian, D.; Davidowitz, T.; Benoliel, R. The Distribution of Oral Mucosal PH Values in Healthy Saliva Secretors. *Oral Dis.* **2006**, *12* (4), 420−423.
(82) Mura, S.; Manconi, M.; Sinico, C.; Valenti, D.; Fadda, A. M. Penetration Enhancer-Containing Vesicles (PEVs) as Carriers for Cutaneous Delivery of Minoxidil. *Int. J. Pharm.* **2009**, *380* (1−2), 72−79.
(83) Tuğcu-demiröz, F. Development of in Situ Poloxamer-Chitosan Hydrogels for Vaginal Drug Delivery of Benzydamine Hydrochloride: Textural, Mucoadhesive and in Vitro Release Properties. *Marmara Pharm. J.* **2017**, *21* (4), 762−770.
(84) Inal, O.; Alğin Yapar, E. Effect of Mechanical Properties on the Release of Meloxicam from Poloxamer Gel Bases Inal and Yapar: Mechanical Properties on Meloxicam Gels. www.ijpsonline.com.

https://doi.org/10.1021/acsomega.4c08967
ACS Omega 2025, 10, 5668−5685